



In silico predictions of gastrointestinal drug absorption in pharmaceutical product development: Application of the mechanistic absorption model GI-Sim



Erik Sjögren^a, Jan Westergren^b, Iain Grant^c, Gunilla Hanisch^d, Lennart Lindfors^d, Hans Lennernäs^a, Bertil Abrahamsson^d, Christer Tannergren^{d,*}

^a Department of Pharmacy, Uppsala University, BOX 580, S-751 23 Uppsala, Sweden

^b Wendelsbergs beräkningskemi AB, Kyrkvägen 7B, S-435 35 Mölnlycke, Sweden

^c Pharmaceutical Development, AstraZeneca R&D Alderley Park, UK

^d Pharmaceutical Development, AstraZeneca R&D Mölndal, Sweden

ARTICLE INFO

Article history:

Received 14 March 2013

Received in revised form 24 April 2013

Accepted 14 May 2013

Available online 29 May 2013

Keywords:

Solubility

Intestinal permeability

Absorption modeling

In silico prediction

Fraction absorbed

ABSTRACT

Oral drug delivery is the predominant administration route for a major part of the pharmaceutical products used worldwide. Further understanding and improvement of gastrointestinal drug absorption predictions is currently a highly prioritized area of research within the pharmaceutical industry. The fraction absorbed (f_{abs}) of an oral dose after administration of a solid dosage form is a key parameter in the estimation of the in vivo performance of an orally administered drug formulation. This study discloses an evaluation of the predictive performance of the mechanistic physiologically based absorption model GI-Sim. GI-Sim deploys a compartmental gastrointestinal absorption and transit model as well as algorithms describing permeability, dissolution rate, salt effects, partitioning into micelles, particle and micelle drifting in the aqueous boundary layer, particle growth and amorphous or crystalline precipitation. Twelve APIs with reported or expected absorption limitations in humans, due to permeability, dissolution and/or solubility, were investigated. Predictions of the intestinal absorption for different doses and formulations were performed based on physicochemical and biopharmaceutical properties, such as solubility in buffer and simulated intestinal fluid, molecular weight, pK_a , diffusivity and molecule density, measured or estimated human effective permeability and particle size distribution. The performance of GI-Sim was evaluated by comparing predicted plasma concentration–time profiles along with oral pharmacokinetic parameters originating from clinical studies in healthy individuals. The capability of GI-Sim to correctly predict impact of dose and particle size as well as the in vivo performance of nanoformulations was also investigated. The overall predictive performance of GI-Sim was good as >95% of the predicted pharmacokinetic parameters (C_{max} and AUC) were within a 2-fold deviation from the clinical observations and the predicted plasma AUC was within one standard deviation of the observed mean plasma AUC in 74% of the simulations. GI-Sim was also able to correctly capture the trends in dose- and particle size dependent absorption for the study drugs with solubility and dissolution limited absorption, respectively. In addition, GI-Sim was also shown to be able to predict the increase in absorption and plasma exposure achieved with nanoformulations. Based on the results, the performance of GI-Sim was shown to be suitable for early risk assessment as well as to guide decision making in pharmaceutical formulation development.

© 2013 Elsevier B.V. All rights reserved.

Abbreviations: AAF, area amplification factor; ABL, aqueous boundary layer; ACAT, advanced compartmental absorption and transit; ADAM, advanced dissolution absorption and metabolism; AUC, area under the plasma concentration time curve; API, active pharmaceutical ingredient; BCS, Biopharmaceutics Classification System; BSA, bovine serum albumin; CAT, compartmental absorption and transit; CYP3A4, cytochrome P450 3A4; D , diffusion coefficient in water; F , bioavailability; f_0 , fraction uncharged; f_{abs} , fraction absorbed; $f_{stirring}$, stirring factor; FaSSiF, fasted simulated small intestinal fluid; GI, gastrointestinal; k , Boltzmann's constant; L , aqueous boundary layer thickness; M_w , molar weight; η , viscosity of water; P , permeability; P_{ABL} , permeability in the aqueous boundary layer; P_{app} , Caco-2 apparent permeability; P_{eff} , human effective jejunal permeability; P_m , membrane permeability; ρ , molar density; r , molecule radius; R , particle radius; S , solubility; τ , transit time; V_M , molar volume; q , fraction of dissolved active pharmaceutical ingredient partitioned to micelles.

* Corresponding author. Address: Medicines Evaluation CVGI, Pharmaceutical Development, AstraZeneca R&D Mölndal, Pepparedsleden 1, 431 83 Mölndal, Sweden. Tel.: +46 (0)31 776 1976; fax: +46 (0)31 776 3834.

E-mail address: christer.tannergren@astrazeneca.com (C. Tannergren).

1. Introduction

Sufficient intestinal absorption is a prerequisite for the successful development of an oral drug product when a systemic effect is a desired. The fraction absorbed (f_{abs}) of an oral dose after administration of a solid dosage form is a key parameter in the estimation of the in vivo performance of an oral formulation and it is generally thought to be determined by the interplay between solubility in relation to dose and intestinal permeability, in accordance to the Biopharmaceutics Classification System (BCS) (Amidon et al., 1995). However, the gastrointestinal absorption process is in reality a complex process determined by the physicochemical and biopharmaceutical properties of the active pharmaceutical ingredient (API) as well as formulation and physiological factors (Löbenberg and Amidon, 2000). In contrast to the available in vitro models, a mechanistic physiologically based absorption model taking all these aspects into account would have the potential to improve the understanding of the factors limiting the intestinal absorption and enable prediction of rate and extent of absorption in humans. This is also why an increased use of model based research has been encouraged and emphasized by regulatory authorities (Jiang et al., 2011; Jönsson et al., 2012; Zhao et al., 2012). To provide accurate and reliable predictions of f_{abs} in humans, an in silico absorption model needs to combine appropriate equations describing processes like membrane permeation, solubility, dissolution, partitioning into micelles, particle size, particle growth and precipitation with an appropriate description of the physiology in different regions of the gastrointestinal tract, such as fluid volumes, transit times, areas and luminal pH (Sugano, 2009). In order to better visualize the output the absorption model can preferably be linked to a pharmacokinetic (PK) model to enable modeling and simulation of plasma concentration–time profiles.

To date, a number of mechanistic models for the prediction of intestinal absorption have been published and several commercial software are currently available: GastroPlus™, which is based on the advanced compartmental absorption and transit (ACAT) model, an extension of the original compartmental absorption and transit (CAT) model; Simcyp®, which is based on the advanced dissolution absorption and metabolism (ADAM) model and PK-SIM® (Agoram et al., 2001; Darwich et al., 2010; Sugano, 2009; Thelen et al., 2011; Yu et al., 1996). These models have been shown to be useful in the predictions of f_{abs} and plasma exposure of drugs (Parrott and Lave, 2008; Sugano, 2011). However, in some studies the accuracy in the in silico predictions based on in vitro data has been less satisfying, e.g., only 11% of predictions of the AUC in humans after oral dosing were made within a 2-fold prediction error (Poulin et al., 2011). Limitations in prediction of absorption was hypothesized to be a major reason for the disappointing results since prediction of intravenous data and associated disposition PK parameters was much better (Poulin et al., 2011). In addition, there are still considerable gaps for appropriate descriptions of processes related to colonic absorption and in vivo precipitation as well as predictions of the in vivo performance of nanoformulations (Kesisoglou and Wu, 2008).

A major biopharmaceutic and formulation development related challenge during recent years has been the increased number of low solubility APIs. These molecules are associated with an increased risk for solubility and dissolution limited intestinal absorption with resulting effects such as particle size-dependent absorption, significant food effects and dose-dependent (less than linear) PK. It has been estimated that as many as 90% of the new candidate entities are classified as BCS Class II or IV (Benet et al., 2006). As there also is a demand to reduce development times and increase cost-effectiveness there is a clear need of in silico

absorption models with the capability to accurately predict solubility/dissolution limited absorption. This also includes the potential impact that modifications to the solid state form, such as polymorphism, amorphicity and salts may have on the absorption rate, f_{abs} and bioavailability (F) of the API. Reliable predictions on these aspects would be most valuable to guide formulation development, e.g., enabling rational decisions for particle size reduction and/or identifying a need for solubility enhanced formulation. To address these challenges an absorption simulation software named GI-Sim has been developed within AstraZeneca. GI-Sim is based on the CAT model but further developed with appropriate scientific theories describing the events in the gastrointestinal lumen.

The main objective of this study was to describe the gastrointestinal absorption model GI-Sim and to evaluate the prediction accuracy of f_{abs} and the plasma PK for drugs with incomplete intestinal absorption in humans. Special emphasis was put on APIs with known solubility/dissolution limited absorption, which display dose and/or particle size dependent absorption. In addition, the capability of GI-Sim to correctly predict in vivo performance of nanoformulations was also investigated.

2. Material and methods

2.1. The GI-Sim absorption model

GI-Sim deploys a compartmental physiological model for the gastrointestinal tract together with a compartmental PK model, with the possibility to use up to three compartments, to describe the plasma concentration–time profile. The physiological model adopted in GI-Sim constitutes of nine gastrointestinal compartments coupled in series; the stomach (1), the small intestine (2–7) and the colon (8–9) (Fig. 1). The description of the underlying physiology has been reported previously (Yu and Amidon, 1998, 1999; Yu et al., 1996).

In GI-Sim, the intestinal content flows from one compartment to the next bringing dissolved API molecules and undissolved material. In contrast, bile salt micelles are modeled with a constant concentration in each compartment. Each compartment is assumed to be ideal, i.e. concentrations of dissolved and undissolved API, pH, etc. are the same throughout the compartment, apart from a thin aqueous boundary layer (ABL) at the intestinal wall. Each compartment has a specific biorelevant pH and as a consequence the solubility of ionisable APIs changes along the gastrointestinal tract. The key processes to the absorption, i.e., permeability, solubility, dissolution/precipitation and molecular nucleation, are described in Section 3. Theory. GI-Sim also comprises other functionalities such as luminal degradation, API release profiles e.g. for controlled release formulations and physiology models for pre-clinical species. However, these aspects were beyond the scope of this study and are therefore not described further.

For an ideal gastrointestinal compartment with transit time (τ), the amount of API leaving the compartment to the compartment downstream during unit of time is

$$F_{outflow} = \frac{X}{\tau} \quad (1)$$

where F represent the flow (amount/time) and X is the amount of API present in the compartment. The amount of API leaving one compartment instantaneously enters the next one. Within a compartment particles may either dissolve or grow and dissolved API may partition into the bile salt micelles or be transported across the intestinal membrane. In this study it was assumed that once a molecule has been absorbed no transport back into the lumen is possible. In GI-Sim, micelles are present in the intestinal compartment

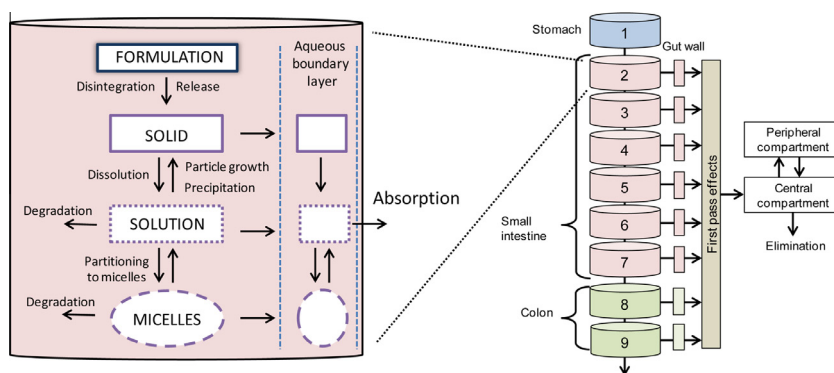


Fig. 1. GI-Sim. A schematic view of the absorption model GI-Sim. To the left a representation of the processes occurring in each compartment is shown. To the right, the nine ideal GI-compartments of the gastrointestinal tract linked with first pass effects and a pharmacokinetic two-compartmental model is shown.

2–7, representing the small intestine, to mimic the bile secretion in duodenum (intestinal compartment 2) and the reabsorption of bile salts in the distal ileum (intestinal compartment 7).

Physiological parameters for the different GI regions such as volumes, transit times and pH in the intestinal media were adopted from Heikkinen et al. (2012). The area available for absorption in each compartment ($A_{\text{compartment}}$) was calculated, assuming an ideal tube, from the compartment volumes and a mean radius (weighted by the segments length) of 1.15 cm. This was based on the assumption that the fluid into the GI tract is distributed as small segments from where the absorption occurs, i.e., there are parts along the intestine with no fluid where absorption does not take place (Schiller et al., 2005). Moreover, even if the intestine can be depicted as a tube, certain structures, such as folding, villi and microvilli, also affects the available area for absorption. This was accounted for in GI-Sim by using an area amplification factor (AAF) ranging from 3 in the proximal small intestine to 1 in the distal small intestine which previously has been stated to be physiologically relevant (Mudie et al., 2010; Willmann et al., 2004). The AAF for respective compartment was based on the length of the segments and mean distance from the proximal end of the small intestine.

The mass transport, $F_{\text{absorption}}$, of free dissolved API molecules across the intestinal membrane in each compartment is proportional to permeability (P), the free concentration in the bulk (C_b), and the surface area available for absorption (SA; $SA = A_{\text{compartment}} \cdot AAF$) according to

$$F_{\text{absorption}} = P \cdot C_b \cdot SA \quad (2)$$

The adoption of C_b in Eq. (2) rather than the concentration difference over the membrane is appropriate when the blood on the basolateral side of the membrane is regarded as an ideal sink. Extensive and well characterized human P measurements are only available from the jejunum. Hence, the human effective jejunal permeability (P_{eff}) was also implemented for duodenum and ileum although regional differences are acknowledged. In this study, it was assumed that no absorption occurs from the two colon compartments since the physiology in the colon is less well defined scientifically and that a general overprediction of the absorption of solubility limited drugs has been reported (Kesisoglou and Wu, 2008).

After absorption, the API may be metabolised during the passage over the intestinal wall and through the liver before reaching the systemic circulation. The combined contribution of these two processes is estimated as a first pass effect factor. The concentration–time profile in the systemic circulation in GI-Sim is described by one, two or three compartment kinetics with a clearance from the central compartment. An overview of the flows and processes in GI-Sim are schematically shown in Fig. 1.

The fluid in the small intestine, relevant for intestinal compartments 2–7, contains bile salts and phospholipids that together form mixed colloidal structures (Mazer et al., 1980; Persson et al., 2005). A majority of these aggregates are small at physiological conditions, i.e., micelles and vesicles (Müllertz et al., 2012; Nawroth et al., 2011). A colloidal particle size of 6 nm was adopted in GI-Sim and these structures will hereafter be referred to as micelles even though the presence of other structures is acknowledged. Estimation of the total micellar volume was made on basis on the constituents concentrations and molecular descriptors (molar weight (M_w), molar volume (V_M), molecular density) along with a micellar composition of bile salt:phospholipid ratio equal to 1:2 (Mazer et al., 1980). A micellar volume fraction of 0.0002 was calculated and implemented in the model based on the following information of the intestinal fluid composition: taurocholate (0.048 mM, $M_w = 515.7$ g/mol, $V_M = 407.7$ cm³/mol), glycocholic acid (0.073 mM, $M_w = 465.6$ g/mol, $V_M = 383.7$ cm³/mol), taurochenodeoxycholic acid (0.043 mM, $M_w = 499.7$ g/mol, $V_M = 358.8$ cm³/mol), glycochenodeoxycholic acid (0.030 mM, $M_w = 449.6$ g/mol, $V_M = 386.8$ cm³/mol) and phospholipids (assumed to be lecithin predominately) (0.2 mM, molecular density = 1.04 g/cm³) (Persson et al., 2005). The physiological parameters in GI-Sim are summarized in Table 1.

2.2. Physicochemical properties

The fundamental physicochemical properties needed for the predictions of intestinal absorption in GI-Sim were pK_a , V_M , M_w , solubility (S) and the diffusion coefficient in water (D). pK_a was either collected from the literature or experimentally determined using appropriate methodologies. V_M was estimated using the software ACD/Labs v. 12.0 (Advanced Chemical Development Inc, Toronto, Canada). V_M and M_w were used for the calculation of molar

Table 1
Physiological parameters for a 70 kg human in the fasted state.

	Volume (ml)	Transit time (min)	pH	Volume fraction micelles	SA (cm ²)
Stomach	47	15	1.3		
Duodenum	42	16	6.0	0.0002	160
Jejunum 1	150	56	6.2	0.0002	580
Jejunum 2	120	44	6.4	0.0002	440
Ileum 1	94	35	6.6	0.0002	330
Ileum 2	71	25	6.9	0.0002	230
Ileum 3	50	17	7.4	0.0002	150
Colon 1	47	250	6.4		28
Colon 2	50	750	6.8		42

Table 2
APIs and data used for the construction of the $P_{m-human} - P_{m-caco-2}$ correlation.

	P_{eff} (10^{-4} cm/s)	$P_{ABL-human}^a$ (10^{-4} cm/s)	$P_{m-human}^a$ (10^{-4} cm/s)	P_{app} (10^{-4} cm/s)	$P_{ABL-caco-2}^b$ (10^{-4} cm/s)	$P_{m-caco-2}^b$ (10^{-4} cm/s)	$\log P_{m-human-f}^c$	$\log P_{m-caco-2-f}^c$
Carbamazepine	4.3	9.1	8.2	0.36	2.6	0.42	0.91	-0.38
Cimetidine	0.26	8.9	0.27	0.0055	2.6	0.0055	-0.12	-1.8
Desipramin	4.5	8.2	10	0.16	2.4	0.17	4.3	2.5
Furosemide	0.05	8.8	0.05	0.002	2.5	0.002	1.7	0.29
Hydrochlorothiazide	0.04	9.3	0.04	0.003	2.7	0.003	-1.4	-2.5
Inogatran	0.03	7.6	0.03	0.00061	2.2	0.00061	-1.5	-3.2
Metoprolol	1.34	8.2	1.6	0.13	2.3	0.14	2.9	1.8
Piroxicam	6.65	8.7	28	0.91	2.5	1.4	2.6	1.3
Propranolol	2.91	8.4	4.5	0.18	2.4	0.19	3.3	2.0

^a $P_{ABL-human}$ and $P_{m-human}$ was calculated assuming an aqueous boundary layer of 86 μ m.

^b $P_{ABL-caco-2}$ and $P_{m-caco-2}$ was calculated assuming an aqueous boundary layer of 300 μ m.

^c $P_{m-human}$ and $P_{m-caco-2}$ compensated for fraction uncharged (f_0) at pH = 6.5.

density (ρ ; $\rho = M_w/V_M$). D was estimated by Stoke–Einstein's equation,

$$D = \frac{k \cdot T}{6 \cdot \pi \cdot \eta \cdot r} \quad (3)$$

where k is the Boltzmann's constant, T is the absolute temperature, η is the viscosity of water and r is the molecule radius, given by V_M .

2.3. Solubility data

Solubility data used for the study APIs in phosphate buffer pH = 6.5 and fasted simulated small intestinal fluid (FaSSIF) at 37 °C was either obtained from previous work performed within AstraZeneca by Söderlind et al. or determined using the same methodology described in their report (Söderlind et al., 2010). The volume fraction of micelles in FaSSIF was calculated, as described in Section 2.1, to a value of 0.0007 based on the taurocholate and lecithin concentrations 0.375 mM (total concentration 3 mM) and 0.75 mM, respectively (Söderlind et al., 2010). The partitioning to micelles can be determined using measured API solubility in buffer and FaSSIF at the same pH and knowing the micellar volume fraction in FaSSIF. The partitioning of API in intestinal fluid can then be calculated by the micellar volume fraction in intestinal fluid and assuming equivalent micelle composition and micellar partitioning of API as in FaSSIF. The difference between the volume fraction of micelles in FaSSIF (0.0007) and intestinal fluid (0.0002) was automatically accounted for in the simulations by GI-Sim.

2.4. Permeability data

When available, previously reported P_{eff} values were used as permeability input in the simulations for all regions in the small intestinal (Lennernäs, 2007). In the absence of such data, the human P_{eff} was estimated from an established correlation between P_{eff} and Caco-2 apparent permeability (P_{app}). Briefly, the Caco-2 permeability experiments were performed manually in the apical-basolateral direction in 12 or 24 well plates (1.13 cm² filters) on a thermostated shaker at 37 °C at a stirring rate of 450 rpm. Details of the experimental procedure are described elsewhere (Hayashi et al., 2008). For APIs with suspected adsorption to plastics and/or intracellular retention, 4% bovine serum albumin (BSA) was added on the basolateral side to obtain sink conditions and sufficient recovery.

2.5. Estimation of human P_{eff} from Caco-2 in vitro P_{app}

As a consequence of inadequate stirring the Caco-2 assay generally suffers from thicker ABL, and hence a greater resistance from the ABL, than in the in vivo intestinal environment (Fagerholm and Lennernäs, 1995; Karlsson and Artursson, 1991). For this

reason, the correlation between P_{eff} and P_{app} was established assuming a linear relation between the membrane permeability (P_m) in humans ($P_{m-human}$) and the P_m for the Caco-2 cell membrane ($P_{m-caco-2}$). P_m can be calculated if the permeability in the ABL (P_{ABL}) is known. For a solution P_{ABL} can be attained via knowledge of the aqueous boundary layer thickness (L) and D (see Section 3.2 Membrane and intestinal permeability). The L in vivo ($L_{in vivo}$) was estimated to 86 μ m based on the observed P_{eff} for ketoprofen ($P_{eff} = 8.7 \times 10^{-4}$ cm/s), which is the API with the highest human P_{eff} , under the assumption that the membrane resistance for this molecule is negligible compared to the resistance in the ABL and applying an estimated value of D ($D_{ketoprofen} = 0.749 \times 10^{-9}$ m²/s). Estimation of L for the used Caco-2 model (L_{caco-2}) was based on P_{app} measurements for felodipine in solution ($P_{app} = 220 \times 10^{-6}$ cm/s) and as a saturated nanosuspension ($P_{app} = 1100 \times 10^{-6}$ cm/s). Assuming that the permeability through the ABL in the latter case is infinite yields a L_{caco-2} of 240 μ m. However, since the permeability through the ABL is limited in the nanoparticle case L_{caco-2} must be greater than 240 μ m and a value of 300 μ m was used. Applying these estimates of $L_{in vivo}$ and L_{caco-2} , $P_{m-human}$ and $P_{m-caco-2}$ was calculated for a set of APIs with published P_{eff} values and Caco-2 P_{app} measurements. A log–log relationship was then established for $P_{m-human}$ and $P_{m-caco-2}$, compensated for fraction uncharged (f_0) at pH 6.5, which was thereafter used for predictions of P_{eff} from P_{app} measurements. APIs and the data used to attain the $P_{m-human} - P_{m-caco-2}$ correlation is reported in Table 2 and the $P_{m-human} - P_{m-caco-2}$ correlation is shown in Fig. 2.

3. Theory

A schematic mathematical description of the GI-Sim model is given in Appendix A. This description is for the case when all particles are considered monodisperse.

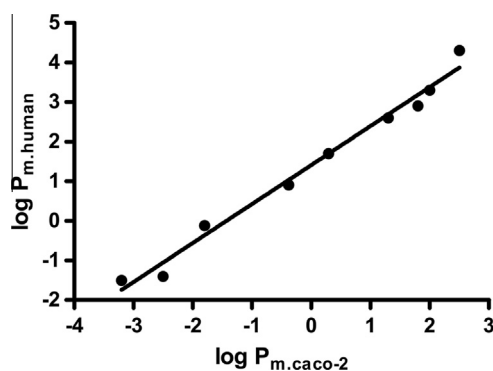


Fig. 2. Caco-2 – human effective jejunal permeability correlation. $P_{m-human} - P_{m-caco-2}$ correlation used to predict P_{eff} from Caco-2 P_{app} measurements. All P_m values were compensated for the fraction uncharged (f_0) at pH = 6.5.

3.1. Solubility, dissolution, particle growth and nucleation

The total solubility, defined as the sum of free monomer and micelle bound molecules per volume media, is in many cases influenced by the pH and the presence of micelles in the media. In GI-Sim the influence of pH on the net charge of acidic and basic APIs was described according to the traditional Henderson–Hasselbalch equation (Henderson, 1908). For APIs with more than one functional group the protonation/deprotonation of each group was assumed to be independent of each other. The concentration of uncharged API at saturation is the intrinsic crystalline solubility (S_0). The solubility in the bulk (S_b) at given pH was directly correlated to S_0 and charge according to

$$S_b = \frac{S_0}{f_0} \quad (4)$$

where f_0 is the fraction of uncharged molecules. A net neutral zwitterion was considered uncharged.

In presence of micelles the concentration of dissolved API as free monomer was denoted C_b . The partitioning of API into and from micelles was assumed to be immediate and the relation between the total concentration (C_t) and C_b could consequently be regarded as proportional at all times. C_t , including the API contained by the micelles, is always proportional to C_b according to

$$C_b = (1 - q) \cdot C_t \quad (5)$$

where q is the fraction of dissolved API partitioned into the micelles. The partitioning of charged molecules into micelles was assumed to be negligible. Hence, for ionized molecules q is dependent of the pH in the small intestine, i.e., it is directly proportional to f_0 .

In analogy with Eq. (5) the total solubility S_t relates to S_b by

$$S_b = (1 - q) \cdot S_t \quad (6)$$

The solubility also influences the dissolution rate and rate of precipitation. In this study, particles were considered to be crystalline and spherical. In GI-Sim, the dissolution rate for a particle in unstirred water is assumed to be driven by diffusion only. Under the assumption of negligible contribution of convection to the dissolution process, the dissolution rate, given as amount of molecules per unit of time, can then be described by Fick's law

$$F_{dissolution} = 4 \cdot \pi \cdot R \cdot D \cdot (S_b - C_b) \quad (7)$$

where R is the particle radius and D is the diffusion coefficient for the API in water. In GI-Sim it is assumed that the rate is controlled by the difference $S_b - C_b$, rather than the difference $S_t - C_t$.

The rate of crystalline nucleation, i.e. the initial step in molecule precipitation from a supersaturated solution, is modeled in GI-Sim by a modified version of the crystalline nucleation theory previously described in detail (Lindfors et al., 2008). Briefly, the nucleation rate is determined by the combination of creation of stable critical clusters of molecules and the transport of free monomer molecules to these clusters. Several parameters such as the level of supersaturation (given by C_b and S_0), D , V_M , q , f_0 as well as the interfacial tension are determinants for the estimation of nucleation rate in this theory. The interfacial tension can be estimated from experimental in vitro precipitation data (Carlert et al., 2010).

In contrast to particle dissolution, it has been noticed that particle growth is slower than obtained by Fick's law as surface integration processes slows down the growth (Lindfors et al., 2008). This is modeled by multiplying the Fick's law rate by the empirical expression $\psi = R/(R + 5 \mu\text{m})$.

The stirring in the compartments leads to increased dissolution and growth rates. Nielsen introduced the stirring factor ($f_{stirring}$), given by Eq. (8), by which the rate is increased (Nielsen, 1961).

$$f_{stirring}(R) = \left[1 + \frac{2 \cdot g \cdot R^3 \cdot (\rho_{drug} - \rho_{water})}{9 \cdot D \cdot \eta_{water}} \right]^{0.285} \quad (8)$$

where g is the gravity constant. The relationship indicates that particle size amplifies $f_{stirring}$ and that $f_{stirring} \approx 1$ for particles with a radius less than $1 \mu\text{m}$. The total dissolution and growth rates are hence described as

$$\begin{cases} F_{dissolution} = 4 \cdot \pi \cdot R \cdot D \cdot (S_b - C_b) \cdot f_{stirring} \\ F_{growth} = -4 \cdot \pi \cdot R \cdot D \cdot (S_b - C_b) \cdot \Psi \cdot f_{stirring} \end{cases} \quad (9)$$

Polydistributions of particles are described by the function $f(R)$ where

$$\int_{R_1}^{R_2} f(R) dR \quad (10)$$

is the number of particles with radius between R_1 and R_2 . Numerically, the size distribution is split up into 20 bins. The time evolution of the distribution is calculated by changing the particle size range of every bin according to Eq. (9). Particles will in this way stay in their original bin. However, the altitude of each bin is changed in order to conserve the number of particles in respective bin. When there is an inflow of particles, the size distribution of a compartment must cover the whole size range in the upstream compartment. In the case when the solubility and consequently the dissolution rate are much lower in the upstream compartment, new empty bins must constantly be added to the size distribution to manage the particle inflow.

3.2. Membrane and intestinal permeability

In GI-Sim, the total transcellular mass transport across the apical membrane of the enterocyte is described by Eq. (2). In order for a molecule to be transported from the intestinal lumen to the blood system it must pass through the epithelial cell layer from the apical surface to the basolateral surface. The epithelial barrier can be depicted as a membrane with an adjacent ABL where the convection of the intestinal water is absent, through which a molecule must diffuse. In GI-Sim, the API transport process from the lumen is modeled as a serial diffusion flow through the ABL of thickness L , with permeability P_{ABL} , and a membrane, with the permeability P_m . Together they constitute a barrier to membrane transport and absorption with the total permeability P , i.e., P_{eff} or P_{app} . P can hence be described by

$$\frac{1}{P} = \frac{1}{P_m} + \frac{1}{P_{ABL}} \quad (11)$$

If the medium in the intestine is a plain solution of API, i.e., no drug particles or API partitioned to micelles, the P_{ABL} is described by Eq. (12) according to Fick's law of diffusion.

$$P_{ABL} = \frac{D}{L} \quad (12)$$

However, when API is present in solid form and/or is partitioning into to the micelles, this theory is inaccurate. Since micelles containing API also diffuse across the ABL, with the diffusion coefficient D_{mic} , they also contribute to the effective transport. It is also assumed that only free molecules in the aqueous phase and no micelles or API in the micelles can enter or penetrate the cellular membrane. To account for the micelle diffusion, P_{ABL} can then be described by

$$P_{ABL} = \frac{D_{mic} \cdot q + D(1 - q)}{L} \quad (13)$$

Generally, for APIs that partition into the micelles ($q > 0$), P_{ABL} will be greater in the presence of micelles than without.

Undissolved drug particles diffuse slower than free API monomers across the ABL but contain many molecules and may therefore contribute substantially to the P_{ABL} . Two processes for the particles are considered in the ABL: particle diffusion and dissolution. If the number of particles is high they may diffuse all the way to the ABL-membrane interface. Otherwise, the region close to the ABL-membrane interface contains no particles. As small and large particles both have different dissolution rate and diffusion rate it is important to consider the size distribution of the particles throughout the boundary layer. In GI-Sim, the diffusion coefficient of particles across the ABL is inversely proportional to the particle radius in accordance to Stoke–Einstein's equation (Eq. (3)). The general effect of particles is that P_{ABL} increases with increasing concentration of particles. This effect will be especially important for small nanosized particles and contribute to the improved absorption provided by such formulations.

The equations above assume that all dissolved molecules are uncharged. For an ionisable molecule, only a fraction (f_0) will be uncharged in the gastrointestinal pH range. Assuming that ionized API molecules have the same diffusion coefficient in water as neutral ones, the P_{ABL} may still be described by Eq. (13). The fact that considerably fewer API monomers partition into the micelles when ionized is taken into account by the change of q . Also, in general the P_m of charged molecules is considered to be minimal in comparison to the uncharged (Hogben et al., 1959). Hence, GI-Sim assumes that molecules with a net charge do not contribute to P_m and that the concentration available for drug transport can be described by $f_0 \cdot C_b$. Altogether the effective permeability in GI-Sim is described by

$$\frac{1}{P} = \frac{1}{f_0 \cdot P_m} + \frac{1}{P_{ABL}} \quad (14)$$

Table 3
APIs with measured human effective jejunal permeability (P_{eff}) values using the Loc-I-Gut technique (Lennernäs, 2007). Collate of physicochemical properties, permeability and observed and GI-Sim predicted fraction absorbed (f_{abs}).

	Mw (g/mol)	pK _a 1 ^a	pK _a 2 ^a	D (10 ⁻⁹ m ² /s)	P_{eff} (10 ⁻⁴ cm/s)	P_{ABL}^b (10 ⁻⁴ cm/s)	P_{mem}^b (10 ⁻⁴ cm/s)	f_{abs} (%)	$f_{abs-pred}$ (%)
α-Methyl dopa	211.2	8.94 b	2.21 a	0.84	0.1	9.8	0.10	55–65	32
Amiloride	229.6	10.2 b	8.65 b	0.94	1.6	11	1.9	80–90	99
Amoxicillin#	365.4	7 b	2.6 a	0.72	0.3	8.4	0.31	45–75	66
Antipyrine	188.2	1.3 b		0.82	5.6	9.5	14	100	100
Atenolol	266.3	9.19 b		0.72	0.2	8.4	0.20	50–60	58
Carbamazepine	236.3	12 a ^c	0.26 b ^c	0.78	4.3	9.1	8.2	>90	100
Cephalexin	347.4	7.05 b	2.55 a	0.73	1.56	8.5	1.9	>90	99
Cimetidine	252.3	6.76 b		0.77	0.26	8.9	0.27	75	60
Cyclosporine	1202			0.42	1.61	4.9	2.4	>90	99
Desipramine HCl	266.4	9.8 b		0.71	4.5	8.2	10	100	100
Enalapril maleate	376.5	5.57 b	2.92 a	0.66	1.57	7.7	2.0	65	99
Enalaprilat	348.4	7.6 b	3.2 a	0.69	0.2	8.0	0.21	8	52
Fexofenadine	501.7	7.84 b ^d	4.2 a ^d	0.59	0.07	6.9	0.07	30–41	24
Fluvastatin sodium	411.5	4.17 a		0.64	2.4	7.5	3.5	95	100
Furosemide	330.8	9.87 a	3.51 a	0.76	0.05	8.8	0.05	40–60	24
Hydrochlorothiazide	297.7	9.78 a	8.53 a	0.80	0.04	9.3	0.04	55	15
Inogatrane	438.6	7.6 b	1.6 a	0.65	0.03	7.6	0.03	5–10	11
Ketoprofen	254.3	4.02 a		0.75	8.7	8.7	5200	100	100
L-dopa	197.2	8.54 b	2.21 b	0.87	3.4	10	5.1	100	100
Lisinopril	405.5	7.01 b	3.16 a	0.65	0.33	7.6	0.34	35–50	69
Losartan	422.9	4.25 a	2.95 a	0.66	1.15	7.7	1.4	100	98
Metoprolol	267.4	9.18 b		0.70	1.34	8.2	1.6	95	98
Naproxen	230.3	4 a		0.77	8.5	9.0	150	100	100
Piroxicam	331.4	5.34 b	1.88 a	0.75	6.65	8.7	28	100	100
Propranolol	259.3	9.17 b		0.72	2.91	8.4	4.5	100	100
Ranitidine	314.4	8 b	2.11 b	0.70	0.27	8.1	0.28	50–60	67
Terbutaline	225.3	9.97 b	8.67 b	0.77	0.3	9.0	0.31	30–73	83
Valacyclovir	324.3	9.23 a	7.4 b	0.75	1.66	8.8	2.0	>80	99
R-verapamil	454.6	8.76 b		0.59	6.8	6.9	520	100	100
S-verapamil	454.6	8.76 b		0.59	6.8	6.9	520	100	100

^a a = acid, b = basic, data from Avdeef and Tam (2010) if not indicated otherwise.

^b Calculated assuming an aqueous boundary layer of 86 μm.

^c Data from Zhang et al. (2011).

^d Data from Yasui-Furukori et al. (2005).

where P_{ABL} is given by Eq. (13) when particles are absent. When particles are present P_{ABL} is obtained numerically and varies with time.

4. Evaluation of GI-Sim

4.1. Sensitivity simulations

A set of simulations was conducted to demonstrate the interplay and effect of both permeability and solubility processes on f_{abs} of the model. The simulations were performed in a permeability and solubility range of 0.08–8 × 10⁻⁴ cm/s and 0.1–100 μg/ml, respectively. Simulations were performed for a theoretical API administered as a suspension ($R = 10 \mu\text{m}$) at a dose of 25 mg together with 200 ml water. At the highest investigated solubility, 100 μg/ml, the dose would hence be completely soluble in the stomach as the total volume at administration will be approximately 250 ml (200 ml + 47 ml (stomach volume)). Molecule properties were set as; neutral, $Mw = 400 \text{ g/mol}$, $D = 0.7 \times 10^{-9} \text{ m}^2/\text{s}$, $S_{FASSIF}/S_{buffer} = 1$, and a molecule density of 1.3 g/ml. The influence of particle size and dose was investigated by changing one of these properties separately from the general setting to following values: particle radius = 0.1 and 100 μm and dose = 250 and 2.5 mg.

4.2. Prediction of f_{abs} for solutions of APIs with known P_{eff}

All APIs with measured human P_{eff} values (range: 0.03–8.7 × 10⁻⁴ cm/s) and reported values of f_{abs} (range: 5–100%) for solutions were used in order to evaluate of how well GI-Sim could describe the membrane permeability process in vivo in humans (Borgström et al., 1989; Kansy et al., 1998; Lancaster and Todd, 1988; Lappin et al., 2010; Lennernäs, 2007). To enable evaluation

Table 4

Model APIs used in the evaluation of GI-Sim and fundamental input to the model such as solubility, permeability and physicochemical properties. For pK_a values, the notation *a* and *b* indicate acid and base, respectively.

	Mw (g/mol)	pK_a	$\log D_{7.4}$	ρ (g/ml)	D (10^{-9} m ² /s)	S_{buffer} (μ g/ml)	S_{FaSSiF} (μ g/ml)	S_{FaSSiF}/S_{buffer}	P_{app} (10^{-4} cm/s)	P_{eff} (10^{-4} cm/s)	BCS	
Aprepitant	534	2.4 b	9.15 a	6.9	1.51	0.63	0.37	23	62	1.7	7.1 ^b	II
Carbamazepine	236	12 a ^e	0.26 b	1.6	1.27	0.78	127	236	1.9	4.3 ^a	II	
Danazol	337	Neutral	3.7	1.21	0.68	0.5	8.7	17	1.7	7.5 ^b	II	
Digoxin	781	Neutral	1.3	1.36	0.54	11.4	14.3 ^c	1.3	0.017	0.41 ^b	II	
Felodipine	384	Neutral	4.3	1.28	0.67	1.0	53	44	2.2	7.8 ^b	II	
Fenofibrate	361	Neutral	6.9	1.18	0.66	0.25	13.7	56	2.2	7.7 ^b	II	
Fexofenadine	502	4.2 a ^e	7.84 b	0.23	1.17	0.59	530 ^d	530	1.0	0.07 ^a	III	
Griseofulvin	353	Neutral	2.9	1.38	0.70	15	20	1.3	1.3	7.3 ^b	II	
Irbesartan	429	4.9 a ^e	1.5	1.31	0.65	102	112	1.1	0.43	4.6 ^b	I	
Ketoconazole	531	2.9 b ^e	6.5 b	4.1	1.38	0.61	6.5	26	4.0	3.3 ^b	II	
AZ1	475 ± 5	Neutral	2.4	1.34	0.63	80	110	1.4	1.2	6.6 ^b	II	
AZ2	545 ± 5	0.75 b	2.74 b	1.5	1.43	0.62	3.7	8.7	2.4	0.019	0.46 ^b	IV

^a P_{eff} measured in vivo.

^b P_{eff} predicted from Caco-2 P_{app} measurement.

^c Measurement performed in human intestinal fluid.

^d Same value as S_{FaSSiF} due to lack of buffer solubility data.

^e pK_a data from Zhang et al. (Carbamazepine), Yasui-Furukori et al. (fexofenadine), Cagigal et al. (Irbesartan) and Skiba et al. (ketokonazole) (Cagigal et al., 2001; Skiba et al., 2000; Yasui-Furukori et al., 2005; Zhang et al., 2011).

of the permeability process only, data for drug solutions where no precipitation was expected was used. Physicochemical properties of the included APIs were collected from the literature or estimated with ACD/Labs. Predicted f_{abs} were compared to published human in vivo data. The input data for the permeability model evaluation is summarized in Table 3.

4.3. Prediction of f_{abs} and plasma exposure of model APIs with limited intestinal absorption in humans

The f_{abs} of twelve APIs (see Table 4) reported to be incompletely absorbed in humans due to permeability, solubility and/or dissolution rate limited absorption was simulated to evaluate the accuracy of the absorption model in GI-Sim regarding prediction of f_{abs} and plasma exposure in humans. This strategy was assumed to provide a more discriminating evaluation of the model rather than inclusion of a larger dataset biased towards a high degree of f_{abs} and thereby less challenging predictions. From an industrial formulation development perspective, it is more useful to be able to predict non-linear plasma exposure and particle size dependence rather than having a f_{abs} correlation based on a large dataset. The evaluation was performed both with respect to capturing plasma concentration–time profiles as well as the ability of GI-Sim to capture the impact on drug exposure caused by changes in dose and/or particle size. Systemic exposure was expressed as the area under the plasma concentration time curve (AUC). The literature was thoroughly searched for suitable clinical studies to be used as references to the predictions. Information of particle size and, when available, particle distribution was gathered from the published reports. In those cases where no information was stated the following procedure was adopted: (1) particle size was considered to be the volume weighted average diameter equal to the value stated for commercial product (2) the particle size distribution was calculated according to the Schultz distribution where the number weighted average diameter was assumed to be half the volume weighted average diameter (Kotlarchyk et al., 1988; Zimm, 1948). A volume weighted average diameter equal to 50 μ m was assumed if no information of particle size could be found (only applied for irbesartan). The volume of water consumed at the oral intake of the dose was adopted as specified in the reference studies and assumed to be 240 ml if not specified. Estimation of appropriate systemic PK parameters was performed on the basis of

intravenous dose data. However, when such information was unavailable or when the risk for non-linear elimination/metabolic kinetic behavior was imminent the estimations were performed on basis of concentration–time profiles after oral administration, preferably solutions. Adopted PK parameters are appended as Supplementary data. Variability, as standard deviation, in observed data was extracted from the included studies when available.

To appropriately estimate in vivo f_{abs} in humans mass balance data is required. In the clinic, it is cumbersome to gather samples that are acquired for calculation of mass balance and generally this is not done, which makes this information rare. Mass balance information was unavailable in the clinical studies included as references in this study. The evaluation was therefore based on AUC as a surrogate endpoint to f_{abs} . The evaluation was performed in three parts. First, a general evaluation of how well GI-Sim could predict plasma exposure (i.e., AUC), C_{max} and t_{max} were performed. In the second part the ability of GI-Sim to capture dependence in dose and particle size, which are key aspects in clinical formulation development, were evaluated. Also, the ability to predict the in vivo performance of nanoformulations was investigated. The rationale for the second part was that an ability to capture trends in dose or particle size dependency would be very helpful in decision-making of new formulation strategies and in absorption risk assessments, even if the total exposure is inaccurately predicted. The result for the second part was assessed by comparison of observed and predicted plasma exposure normalized to dose in combination with the predicted f_{abs} . This approach provides the possibility to analyze if the trend in observed AUC is directly reflected of f_{abs} or if other processes also affect the plasma exposure.

4.4. Model APIs

4.4.1. Aprepitant

The selective neurokinin I receptor antagonist aprepitant is highly lipophilic ($\log D_{7.4} = 6.9$). Based on its low solubility and high permeability it is classified as a BCS Class II drugs. Aprepitant is an ampholyte with a weak basic ($pK_a = 2.4$) and weak acidic ($pK_a = 9.2$) group and is thereby mainly unchanged in the gastrointestinal tract. The solubility in biorelevant media, such as FaSSiF, is considerably higher compared to buffer ($S_{FaSSiF}/S_{buffer} > 50$) indicating significant partitioning into the micelles. Aprepitant is

marketed as a nanoformulation (EMEND®) (Wu et al., 2004). Studies in beagle dogs showed that the plasma exposure was 4-fold higher after oral administration of a nanosuspension (particle size = 0.12 µm) compared to micronised suspension (particle size = 5.5 µm) (Wu et al., 2004). The bioavailability in male volunteers after oral administration of 80 mg and 125 mg IR-capsules containing a nanodispersion was 0.70 and 0.65, respectively (Majumdar et al., 2006). Aprepitant biotransformation is mainly mediated by cytochrome P450 3A4 (CYP3A4) (Sanchez et al., 2004). Reports of clinical drug–drug interactions between aprepitant and known CYP3A4 substrate as well as tendencies of non-linear elimination at increased aprepitant doses indicate the possibility of auto-inhibition (Aapro and Walko, 2010; Sanchez et al., 2004). This might be the explanation to the slight supra proportional dose–exposure relationship reported for 80 mg and 125 mg (Majumdar et al., 2006). Systemic PK parameters for each dose were calculated as data were available for an intravenous dose of 2 mg radio labeled aprepitant co-administered both with the 80 mg and 125 mg dose (Majumdar et al., 2006).

4.4.2. Carbamazepine

Carbamazepine is an antiepileptic drug with a narrow therapeutic window. It is commonly classified as a BCS Class II drug owing to its low aqueous solubility and high permeability ($P_{eff} = 4.3$). Within the pH-range of the GI-tract carbamazepine is neutral. Despite the low solubility, high bioavailability and dose linearity in plasma exposure has been observed for solid formulations indicating that carbamazepine is well absorbed. It is well recognized that carbamazepine is metabolized by CYP3A4 (Kerr et al., 1994). Due to the narrow therapeutic window a variety of different oral formulations has been developed to control the plasma exposure profile (Zhang et al., 2011). Simulations of absorption and plasma concentration–time profiles after administration of 200 mg (suspension, particle size = 5 µm) and 400 mg (IR tablets, particle size = 75 µm) carbamazepine was performed in this study. Reference data were collected from the literature (Kovacevic et al., 2009; Zhang et al., 2011). Data from an intravenous administration could not be found in the literature and for this reason was systemic PK parameters calculated based on the reported 200 mg dose (Zhang et al., 2011).

4.4.3. Danazol

The synthetic androgen danazol is classified as a BCS Class II drug due to its low solubility and high permeability. It is a neutral and highly lipophilic ($\log D_{7.4} = 3.7$) molecule with high degree of partitioning into micelles in biorelevant dissolution media ($S_{FaSSIF}/S_{buffer} > 10$). The reported F of micronized (d50 = 4.46 µm) danazol is low (~10%) (Sunesen et al., 2005). This is generally considered to be caused by a combination of a low f_{abs} and extensive first pass metabolism in gut and liver (Charman et al., 1993). It has been shown that danazol is a substrate and inhibitor of CYP3A4 and it is suggested that the main route of elimination is through hepatic metabolism (Konishi et al., 2001). However, it is also reported that the systemic plasma clearance after intravenous administration is greater than hepatic plasma flow (98 L/h vs. ~54 L/h) and that the F after an oral lipid emulsion is close to 45% (Sunesen et al., 2005). This suggests that other elimination pathways than hepatic metabolism is of importance for the elimination of danazol. In this study, intestinal absorption and pharmacokinetics of a 100 mg and 400 mg (IR-capsule, particle size distribution d10%, d50% and d90%, 1.58 µm, 4.46 µm and 10.2 µm) dose of danazol was simulated and compared to studies in the literature (Hooper et al., 1991; Sunesen et al., 2005). Systemic PK parameters were estimated from available intravenous data (Sunesen et al., 2005).

4.4.4. Digoxin

Digoxin is a cardiac glycoside prescribed to patients with heart failure and arterial fibrillation. The molecule shows low permeability and low solubility but due to the low therapeutic dose compared to the solubility it is classified as a BCS Class III drug. Even though digoxin is neutral and has a M_w of 781 g/mol it is only moderately lipophilic ($\log D_{7.4} = 1.3$) caused by polar molecular structures. This is reflected both in the membrane permeability and that the solubility only is not enhanced by micellar dissolution media ($S_{FaSSIF}/S_{buffer} \approx 1$). Digoxin is readily absorbed (at least 60%) at therapeutic doses (0.4–0.7 mg) and is mainly eliminated through renal filtration and secretion (60–80%) (Ochs et al., 1981). Even if it has been suggested that P-glycoprotein (P-gp) mediated efflux limits the extent of absorption of digoxin, the opposite has also been reported (Chiou et al., 2001; Fenner et al., 2009; Greiner et al., 1999; Igel et al., 2007). Instead, the bioavailability of digoxin have been reported to be significantly increased with particle size reduction (Jounela et al., 1975). Simulations of GI absorption and plasma concentration–time profiles after oral administration of a 0.25 mg dose of digoxin, as a solution and solid formulations (IR-tablets) (particle sizes 13 µm and 102 µm), was performed and compared to reported data (Jounela et al., 1975). Systemic PK parameters were estimated based on plasma concentration–time profiles after intravenous administration (Ochs et al., 1978).

4.4.5. Felodipine

Felodipine is a calcium-antagonist used for the treatment of hypertension. The molecule is, because of its neutral and lipophilic ($\log D_{7.4} = 4.3$) nature, poorly water-soluble and highly permeable and hence classified as a BCS Class II drug. The biorelevant solubility is significantly higher than in buffer ($S_{FaSSIF}/S_{buffer} > 50$) indicating significant partitioning of felodipine into the micelles. Felodipine is completely absorbed when administered as a solution ($f_{abs} \approx 100\%$) (Edgar et al., 1985). However, the F is only 16% due to extensive pre-systemic elimination in gut and liver (Edgar et al., 1985). Felodipine is predominately eliminated by metabolism in the liver and less than 1% is excreted unchanged in urine (Edgar et al., 1985). Significant drug–drug interactions with known CYP3A4 inhibitors have been reported indicating this enzymes clinical importance (Baarnhielm et al., 1986; Jalava et al., 1997). In this study, intestinal absorption and concentration–time profiles following oral intake of solutions (doses 10 mg) or solid formulations (10 mg IR-tablet and 100 mg IR-capsule) was simulated and compared to clinical data. Systemic PK parameters were estimated based plasma concentration profiles after a 3 mg dose administered as an intravenous 10 min infusion.

4.4.6. Fenofibrate

The lipid-lowering agent fenofibrate activates the peroxisome proliferator activated receptor α through its active metabolite fenofibric acid. Fenofibrate is a very lipophilic ($\log D_{7.4} = 6.9$) and neutral molecule with low buffer solubility ($S_{buffer} = 0.25$ µg/ml), which is increased by the presence of micelles ($S_{FaSSIF}/S_{buffer} = 6.3$). Previous studies have reported fenofibrate to be highly permeable and it is consequently classified as a BCS class II drug. The F of a 160 mg dose administered as a nanoformulation has been reported to be approximately 70% (Zhu et al., 2010). In this study, simulations were performed for a micronized formulation (IR-capsule) with a particle diameter of 1.1 µm (dose 160 mg) and a nanosized formulation (IR-tablet) with a particle diameter of 0.2 µm (dose 145 mg) and compared to reported studies (Sauron et al., 2006). The particle size of the microcoated formulation was reported to be about 10 µm (Sauron et al., 2006; Vogt et al., 2008). However, due to the formulations characteristics the dissolution profile was identical with a micronized formulation with a particle size

of 1.1 μm (Vogt et al., 2008). This indicates rapid deagglomeration of the 10 μm particle. Analogous to a previous absorption prediction study by Sugano, a particle size of 1.1 μm were used in the simulations to account for this quality (Sugano, 2011). As fenofibrate is completely biotransformed to fenofibric acid the predicted plasma concentration profiles had to be compared to fenofibric acid plasma concentrations (Weil et al., 1990). The systemic PK input was based on fenofibric acid plasma concentrations profile after a 130 mg dose administered in proximal small bowel (corrected for $F = 87.9\%$) (Zhu et al., 2010).

4.4.7. Fexofenadine

Fexofenadine is a selective non-sedating histamine H_1 receptor antagonist classified as a BCS Class III drug with high solubility and low permeability. Dose–exposure linearity in oral administration has been reported over a range from 0.1 mg to 240 mg (Lappin et al., 2010; Robbins et al., 1998). This indicates that major pharmacokinetic processes, e.g. absorption, distribution and elimination, for fexofenadine are unsaturable in this wide dose range. Fexofenadine is considered to be reasonably metabolic stable although the fraction metabolized after an intravenous dose was reported to be 30% (Lappin et al., 2010). An equally large fraction ($\approx 29\%$) was excreted in bile which indicates that approximately 40% is eliminated through biliary excretion (Lappin et al., 2010). Fexofenadine is known to be a substrate of several uptake and efflux membrane transporter proteins (Ming et al., 2011; Petri et al., 2004; Shimizu et al., 2005). Even as clinical data is ambiguous, the apical efflux protein P-gp has been proposed to play a central role, both in intestinal absorption as well as for biliary excretion (Petri et al., 2006; Tannergren et al., 2003; Uno et al., 2006; Yasui-Furukori et al., 2005). In this study, fexofenadine GI absorption and pharmacokinetics was simulated for oral administration of solutions (doses 0.1, 20, 60, 120 and 240 mg) and tablet (dose 120 mg). The results were compared to data collated from literature (Lappin et al., 2010; Robbins et al., 1998). Systemic PK parameters were estimated based on the plasma concentration profile after administration of an intravenous micro dose (0.1 mg) (Lappin et al., 2010).

4.4.8. Griseofulvin

The antifungal API griseofulvin has been used for systemic treatment of fungal infections in animals and man. It is classified as a BCS Class II drug with low solubility and high permeability. The low solubility is not markedly increased by the presence of micelles in biorelevant media ($S_{\text{FASSTF}}/S_{\text{buffer}} = 1$) despite that griseofulvin is neutral and lipophilic ($\log D_{7.4} = 2.9$). The reported F is low and variable as a consequence of the slow dissolution in the lumen and potential first-pass elimination (Lin and Symchowicz, 1975). Solid dispersion formulations (microsize and ultramicrosize) has been developed and used in commercial products in an attempt to increase the dissolution rate and thereby the fraction absorbed (Straughn et al., 1980). Griseofulvin is completely eliminated through metabolism however the terminal half-life after oral administration is long and variable (9.5–21 h) (Chiou and Riegelman, 1971). Predictions of griseofulvin GI absorption and plasma concentration time-profiles after oral administration of microsize or ultramicrosize particle formulation in the dose range of 250–1000 mg were performed in this study. Reference oral data was collated from published studies (Lin et al., 1973; Marvel et al., 1964). Systemic PK parameters were estimated based on the plasma concentration profile after intravenous administration of 108 mg griseofulvin (Chiou and Riegelman, 1971).

4.4.9. Irbesartan

The angiotensin II receptor antagonist irbesartan is used for treatment of hypertension. The molecule has a low lipophilicity

($\log D_{7.4} = 1.5$) and is regarded as highly permeable. However, despite that the molecular structure includes an acidic moiety ($\text{p}K_a = 4.9$) it has previously been classified as a BCS Class II drug even at intestinal pH due to the relation between solubility ($S_{\text{buffer}} = 102 \mu\text{g}/\text{ml}$) and maximum clinical dose (300 mg). The solubility is not affected by the presence of micelles ($S_{\text{FASSTF}}/S_{\text{buffer}} = 1$). A less than linear increase in exposure with dose has been shown at doses above 600 mg solubility indicating solubility limited GI absorption of the solid formulations (Marino et al., 1998). Irbesartan has a reported F of approximately 60–80% (dose 50–150 mg) and is mainly eliminated unchanged through biliary excretion (Chando et al., 1998; Vachharajani et al., 1998). Simulations of GI absorption and pharmacokinetics after oral administration of 50, 150, 300, 600 and 900 mg irbesartan as tablets was performed in this study and compared to clinical studies (Marino et al., 1998; Vachharajani et al., 1998). No particle size information could be found in the literature. Systemic PK parameters were estimated based on intravenous plasma concentration profiles (Vachharajani et al., 1998).

4.4.10. Ketoconazole

Ketoconazole is an oral antifungal imidazole derivate used for the treatment of systemic fungal infections. It is highly lipophilic ($\log D_{7.4} = 4.1$) and classified as a BCS Class II drug with low solubility and high permeability. Ketoconazole is a diprotic base with $\text{p}K_a$ values within the gastrointestinal pH range ($\text{p}K_{a1} = 2.9$ and $\text{p}K_{a2} = 6.5$). The solubility is enhanced by the presence of micelles ($S_{\text{FASSTF}}/S_{\text{buffer}} = 4$). The relative F of 200 mg dose given as a tablet compared to the same dose in solution was reported to 81%, which indicates that ketoconazole is rapidly dissolved in the stomach (Huang et al., 1986). However, the solubility of ketoconazole in the duodenum is several orders lower than in the stomach, as a result of the difference in pH. This increases the potential for nucleation and particle growth, which indeed has been observed in clinical studies (Psachoulas et al., 2011). Previously published in vitro precipitation data was used to estimate the interfacial tension to a value of 20 mN/m (Edwards et al., 2013). Ketoconazole is eliminated through metabolism as well as an inhibitor of many drug metabolizing enzymes (Badcock et al., 1987; Pelkonen et al., 2008). It has been suggested that ketoconazole inhibits its own metabolism (possible both gut and liver metabolism) as a supra-proportional increase in AUC vs. dose has been observed (Daneshmend et al., 1984). Reference data were collected from the literature and the simulations performed in this study comprised oral administration of 200, 400 and 800 mg ketoconazole both as solution and tablet formulation (Daneshmend et al., 1984; Huang et al., 1986; Otte and Carvajal, 2011). Due to the lack of intravenous data and the presumed auto-inhibition, the systemic PK parameters for each dose were estimated based upon the plasma-concentration time profiles for the oral solutions, after compensation for the predicted f_{abs} , (Huang et al., 1986).

4.4.11. AZ1 and AZ2

Two AstraZeneca investigational APIs were included in the evaluation of GI-Sim. AZ1 is a neutral molecule with moderate buffer solubility of 80 $\mu\text{g}/\text{ml}$ and a high Caco-2 permeability ($P_{\text{app}} = 120 \times 10^{-6} \text{ cm}/\text{s}$). It is lipophilic ($\log D_{7.4} = 2.4$) but do not partition into micelles to a high degree ($S_{\text{FASSTF}}/S_{\text{buffer}} = 1.3$). AZ1 was classified as a BCS Class II drug based on these properties. AZ1 is primarily eliminated through liver metabolism but does not undergo gut wall metabolism. In this study, simulations of an oral micronized suspension at the doses 2, 6, 18, 30, 50, 100 and 180 mg were performed. Predictions of intestinal absorption and plasma concentration–time profiles were compared to observations from a clinical study. Pharmacokinetic parameters were estimated based on plasma-concentration time profiles obtained after intravenous

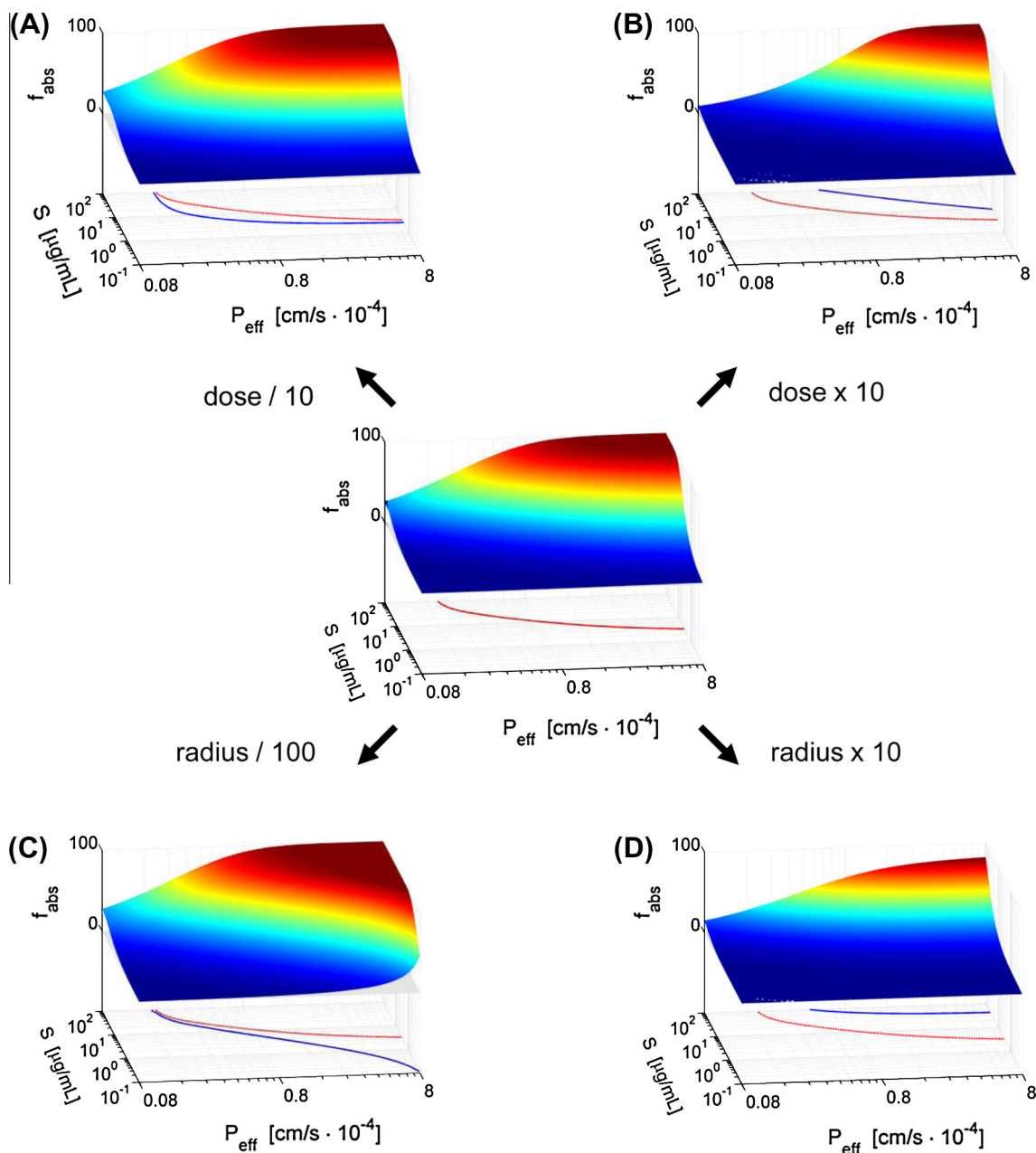


Fig. 3. Sensitivity simulations. The fraction absorbed (f_{abs}) as a function of permeability (P_{eff}) and solubility (S) for a generic API (central plot = default settings) with following properties: neutral, $Mw = 400$ g/mol, $D = 0.7$ (10^{-9} m² s⁻¹), $S_{FaSSIF}/S_{buffer} = 1$, and a molecule density of 1.3 g/ml. The dose (25 mg) was administered as a suspension (particle radius = 10 μ m) given together with 200 ml water. The following changes to the default settings (dose = 25 mg, particle radius = 10 μ m) have been made to the respective plots. (A) Dose = 2.5 mg; (B) dose = 250 mg; (C) particle radius = 0.1 μ m; (D) particle radius = 100 μ m. The blue and red lines indicate where $f_{abs} = 50\%$ at the present and default condition, respectively. (For interpretation of the references to color in this figure legend, the reader is referred to the web version of this article.)

administration. AZ2 is a diprotonic base ($pK_{a1} < 1$, $pK_{a2} = 2.7$) with low solubility ($S_{buffer} = 3.7$ μ g/ml). The solubility is only moderately enhanced by the presence of micelles ($S_{FaSSIF}/S_{buffer} = 2.4$). In vitro studies indicates that it has a low intestinal permeability ($P_{app} = 1.9 \times 10^{-6}$ cm/s) probable due to the low lipophilicity ($\log D_{7.4} = 1.5$) and it is also a substrate for P-gp. The intestinal absorption of AZ2 is solubility limited as no increase of exposure was observed between solid doses of 20 mg and 60 mg. Elimination mainly takes place through hepatic metabolism. AZ2 was classified as a BCS Class IV drug. In this study absorption and pharmacokinetics was simulated after oral administration of 20 and 60 mg AZ2 as a suspension and the result were compared to clinical observations. Pharmacokinetic parameters were estimated

based on plasma-concentration time profiles obtained after intravenous administration.

5. Results and discussion

5.1. Sensitivity simulations

The sensitivity analysis was performed to visualize the response (f_{abs}) of the model to changes in input when both permeability and solubility processes are of importance. The interplay between these two parameters was clearly shown as high permeability facilitated the absorption process at low solubility by maintaining

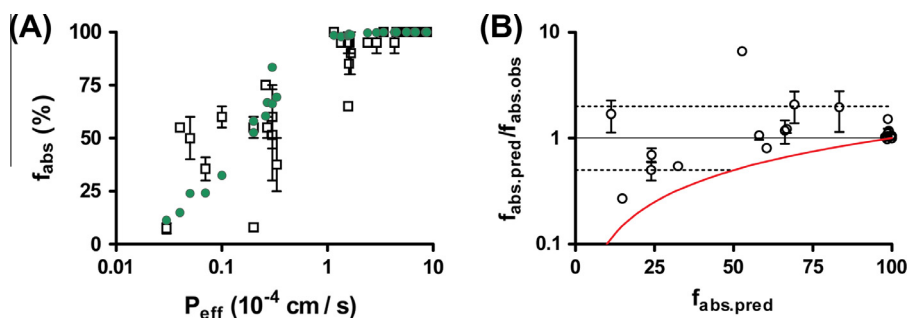


Fig. 4. Absorption prediction of solutions for APIs with measured human P_{eff} . (A) Observed (open squares) and predicted (green circles) f_{abs} of oral solutions for APIs with measured human effective jejunal permeability (P_{eff}) values using the Loc-I-Gut technique. (B) Comparison of predicted and observed f_{abs} . Solid line indicate line of unity, dotted lines indicate a 2-fold deviation. The red line indicates $f_{abs.pred}/100$, i.e., the limit of possible under prediction. (For interpretation of the references to color in this figure legend, the reader is referred to the web version of this article.)

a high concentration gradient in the system. Overall, the simulation exercise showed that a reduction of dose and/or particle size only had a moderately positive effect on the intestinal absorption while an increase of these parameters significantly reduced f_{abs} (Fig. 3). Still, for certain permeability/solubility ranges, a dose and particle size reduction was clearly beneficial for an increased absorption process. Also, it is important to remember the conditions under which the simulations were performed. All simulations, except at the highest level of solubility, were carried out during some level of, initial or continuous, solubility/dissolution limitation to the absorption. The positive effect of a dose reduction (Fig. 3A) was seen in the intermediate permeability range (P_{eff} : 0.2 – 2×10^{-4} cm/s) demonstrating the benefits of an increased solubility to dose ratio. The high dose simulations (Fig. 3B) clearly showed the negative impact on f_{abs} of a reduction of the solubility to dose ratio. Still, high permeability reduced this effect by maintaining the concentration gradient as discussed above. The selected default dose (25 mg) was to be dissolved completely at the highest solubility investigated (100 μ g/ml). This was confirmed by intestinal compartment phase analysis and also through the results observed for the 2.5 mg dose (Fig. 3A). The positive effect on f_{abs} of a particle size in the nano-range (Fig. 3C) was seen at moderate to high permeability ($P_{eff} > 0.8$). This effect is both due to increased dissolution rate and the stipulated theory of small particle diffusion through the ABL. The particle diffusion in ABL increases the API concentration adjacent to the intestinal membrane. This has a significant impact on the effective absorption rate for high permeability APIs but less so for low-moderate permeability APIs. Hence the increased positive effect of a small particle size obtained with increasing permeability. In GI-Sim, the potential benefit of particle size reduction is consequently greater for BCS Class II drugs (low solubility, high permeability) than for BCS Class IV drugs (low solubility, low permeability). The larger particle size (Fig. 3D) significantly decreased the intestinal absorption as a consequence of incomplete and slower dissolution. This dissolution rate limiting effect was most easily observed at $S = 100$ μ g/ml when no impact of solubility limitation was present. The results also indicated that a solubility of approximately 10 μ g/ml could be used as a rough lower limit for high permeability APIs ($P_{eff} > 3$) to obtain acceptable absorption ($f_{abs} = 50\%$). One benefit of this modeling and simulation exercise was the knowledge gained of when, i.e., the APIs characteristics, the model is more or less sensitive to specific input values. It also gave an overall indication when a particle size reduction would be useful or not.

5.2. Absorption prediction of solutions for APIs with determined P_{eff}

The purpose with this part was to evaluate how well GI-Sim could predict f_{abs} when the best possible permeability input was

used, i.e., single-pass measured P_{eff} (Lennernäs, 2007). By comparing predicted to observed f_{abs} after administration of a solution the impact of potential effects related to dissolution as well as particle ABL effects were avoided.

As shown in Table 3 and Fig. 4, there was an overall good agreement between observed and predicted f_{abs} where the difference was less than 10% in 77% (23 of 30) the investigated drugs. The drugs with moderate and high permeability ($P_{eff} > 0.2 \times 10^{-4}$ cm/s) were well predicted with a slight tendency for overprediction of f_{abs} in the moderate permeability region. In contrast, there was a tendency for underprediction of f_{abs} for low permeability molecules ($P_{eff} < 0.2 \times 10^{-4}$ cm/s). Assessment of the accuracy in the predictions, including the limit of possible underprediction, i.e., predicted f_{abs} divided by 100%, is shown in Fig. 4B. Even if the accuracy for APIs with predicted $f_{abs} < 100\%$ is variable it is still shown that 84% (11 of 13) of the predictions were within a 2-fold deviation to the observations. It is important to recognize that the variability in measured P_{eff} and f_{abs} is higher for permeability limited molecules than for highly absorbed drugs, which contribute to the deviations between predictions and measured in vivo data (Hellriegel et al., 1996). It should also be noted that information of micellar partitioning was absent in these predictions. However, it is unlikely that this would have a significant effect on the result since the APIs included in this part of the evaluation, except cyclosporine, are relatively hydrophilic and should therefore theoretically not partition extensively into the micelles. It is also noteworthy that there currently is a lack of measured P_{eff} for highly lipophilic - low solubility APIs. New human permeability data on highly lipophilic molecules would facilitate the development of improved absorption algorithms. Nevertheless, the data presented above show that GI-Sim accurately predicts f_{abs} of solutions for moderate and high permeability molecules but that the model may overemphasize the impact of permeability on f_{abs} for low permeability molecules.

5.3. Prediction of f_{abs} and plasma exposure of model APIs with limited absorption in humans

The purpose of this part was to evaluate how well GI-Sim could predict f_{abs} and plasma exposure in humans for APIs with reported or expected incomplete absorption when administrated as formulations containing solid particles. A compilation of measured and collected input parameters for the model APIs used in the predictions is shown in Table 4. The model APIs included in the evaluation span over a wide range of biopharmaceutical properties (buffer solubility at pH = 6.5: 0.25–530 μ g/ml; S_{FASSIF}/S_{buffer} : 1.3–56; P_{eff} : 0.07 – 7.8×10^{-4} cm/s). The included model APIs also had differences in their physicochemical properties such as ionization (base/acid/neutral), size (M_w) and lipophilicity ($\log D_{7,4}$), which

Table 5
Predictions of f_{abs} and plasma exposure for absorption limited drugs using GI-Sim. Doses, formulations, plasma exposure (observed \pm standard deviation and predicted) and predicted f_{abs} for the reference APIs included in the study. Key processes for limitation of absorption are denoted as follows, permeability (Perm), solubility (Sol) and dissolution (Dis).

Drug	Dose (mg)	Formulation	Particle radius (μm)	AUC _{obs} (ng h/ml)	AUC _{pred} (ng h/ml)	$f_{abs\text{-pred}}$ (%)	Predicted absorption limitation
Aprepitant	80	Nanosuspension	0.06	13,000 \pm 2200	13,300	75	Sol
Aprepitant	125	Nanosuspension	0.06	22,400 \pm 3300	20,600	67	Sol
Ketoconazole	200	Solution	–	15,800 \pm 8300	22,300	49	–
Ketoconazole	200	Tablet	10	14,400 \pm 8200	17,700	39	Sol
Ketoconazole	400	Solution	–	57,300 \pm 15,000	55,200	22	–
Ketoconazole	400	Tablet	10	35,200 \pm 23,000	53,600	21	Sol
Ketoconazole	800	Solution	–	173,000 \pm 39,000	165,000	12	–
Ketoconazole	800	Tablet	10	166,000 \pm 90,000	153,000	11	Sol
AZ2	20	Suspension	2.35	256 \pm 86 ^c	367 ^c	29	Perm/Sol
AZ2	60	Suspension	2.35	336 \pm 150 ^c	409 ^c	11	Perm/Sol
Carbamazepine	200	Suspension	5	149,000 \pm 21,000	149,000	100	–
Carbamazepine	400	Tablet	75	225,000 \pm 56,000	237,000	79	Dis
Danazol	100	Capsule	2.23	136 \pm 68	102	21	Sol
Danazol	400	Capsule	2.23	512 \pm 170	161	8.2	Sol
Griseofulvin	250	Solid	2	13,400 \pm 5300	24,100	84	Sol
Griseofulvin	472	Solid	0.6	30,200 \pm 8100	36,500	68	Sol
Griseofulvin	1000	Solid	3	55,000 \pm 19,000	39,100	34	Sol
Griseofulvin	1000	Solid	8	39,000 \pm 3800	35,200	31	Sol
Felodipine	10	Solution	–	19.6 ^a	18.6	99	–
Felodipine	10	Tablet	2.5	15.3 ^a	14.8	83	Dis
Felodipine	100	Capsule	2.5	50.3 ^a	82.0	49	Sol
AZ1	2	Suspension	2.18	197 \pm 55 ^c	193 ^c	100	–
AZ1	6	Suspension	2.18	466 \pm 80 ^c	582 ^c	100	–
AZ1	18	Suspension	2.18	1480 \pm 240 ^c	1750 ^c	100	–
AZ1	30	Suspension	2.18	3060 \pm 435 ^c	2910 ^c	100	–
AZ1	50	Suspension	2.18	5110 \pm 1900 ^c	4850 ^c	100	–
AZ1	100	Suspension	2.18	6900 \pm 2700 ^c	9700 ^c	100	–
AZ1	180	Suspension	2.18	16,400 \pm 2300 ^c	17,400 ^c	100	–
Digoxin	0.25	Solution	–	4.06 \pm 0.98	7.70	70	Perm
Digoxin	0.25	Solid	6.5	4.03 \pm 0.68	6.89	63	Perm
Digoxin	0.25	Solid	51	1.56 \pm 0.34	1.73	16	Perm/Dis
Fexofenadine	0.1	Solution	–	2.18 \pm 0.38	1.58	24	Perm
Fexofenadine	20	Solution	–	467 \pm 160	316	24	Perm
Fexofenadine	60	Solution	–	1490 \pm 610	949	24	Perm
Fexofenadine	120	Solution	–	2860 \pm 970	1900	24	Perm
Fexofenadine	240	Solution	–	7280 \pm 2500	3790	24	Perm
Fexofenadine	120	Tablet	10	2030 \pm 660	1870	24	Perm
Irbesartan	150	Solution	–	8210 \pm 3500	9100	100	–
Irbesartan	150	Tablet	50 ^b	8610 \pm 4100	8450	84	Dis
Irbesartan	300	Tablet	50 ^b	16,100 \pm 6400	14,200	80	Dis
Irbesartan	600	Tablet	50 ^b	25,100 \pm 14,000	26,100	74	Sol
Irbesartan	900	Tablet	50 ^b	33,300 \pm 23,000	35,900	68	Sol
Fenofibrate	145	Nanosuspension	0.2	120,000 ^a	74,500	40	Sol
Fenofibrate	160	Solid	1.1	100,000 ^a	36,200	17	Sol

^a No variability was available.

^b No particle size information available.

^c AUC values for AZ1 and AZ2 are in arbitrary units due to confidentiality.

indicates that general conclusions likely can be made from this selection of molecules.

5.3.1. Overall predictive performance of GI-Sim

The predicted AUC and f_{abs} for all of the performed simulations of the model APIs are shown in Table 5 and the corresponding observed and predicted plasma profiles are shown in Fig. 5. Since it is difficult to obtain accurate in vivo data of the f_{abs} in humans, the general evaluation was based on prediction of AUC, C_{max} and t_{max} instead, which are well established parameters for this purpose. In general, there was a good agreement between observed and predicted AUC and C_{max} , while there was a somewhat poorer correlation for t_{max} (Fig. 6). The predicted plasma AUC was within one standard deviation of observed mean plasma AUC in 74% (29 of 39) of the simulations (Table 5 and Fig. 5). The accuracy in predictions was categorized into four levels depending on the deviation (observation–prediction): high ($\leq 25\%$ deviation), medium (25–50% deviation), low (50%–2-fold deviation) and inaccurate (> 2 -fold deviation). Based on this, accuracy in the AUC predictions

were high, medium and low in 58%, 15% and 22% of the simulations. In total 95% was within a 2-fold prediction error (Table 6). The predictions of C_{max} was slightly less accurate regarding the highest level but equivalent to the AUC predictions in general as 73% was within 50% deviation and 90% of the cases was within a 2-fold prediction error (Table 6). Ketoconazole solutions as well as carbamazepine at the dose of 200 mg were excluded from this evaluation as the PK parameters were based upon the observed plasma concentration–time profiles from these administrations. No general trend was observed in the predictive power of GI-Sim between neutral, acidic or basic APIs.

The data presented above shows that GI-Sim predicts AUC, and thus f_{abs} , with a high level of accuracy. This makes the model suitable to use in early API absorption risk assessment and in predictions of in vivo performance of different formulations, especially as no model adjustment or data fitting was used in this investigation. It also indicates that GI-Sim performs well compared to other absorption simulation software where the predictive performance, as a 2-fold deviation to observation, has been reported.

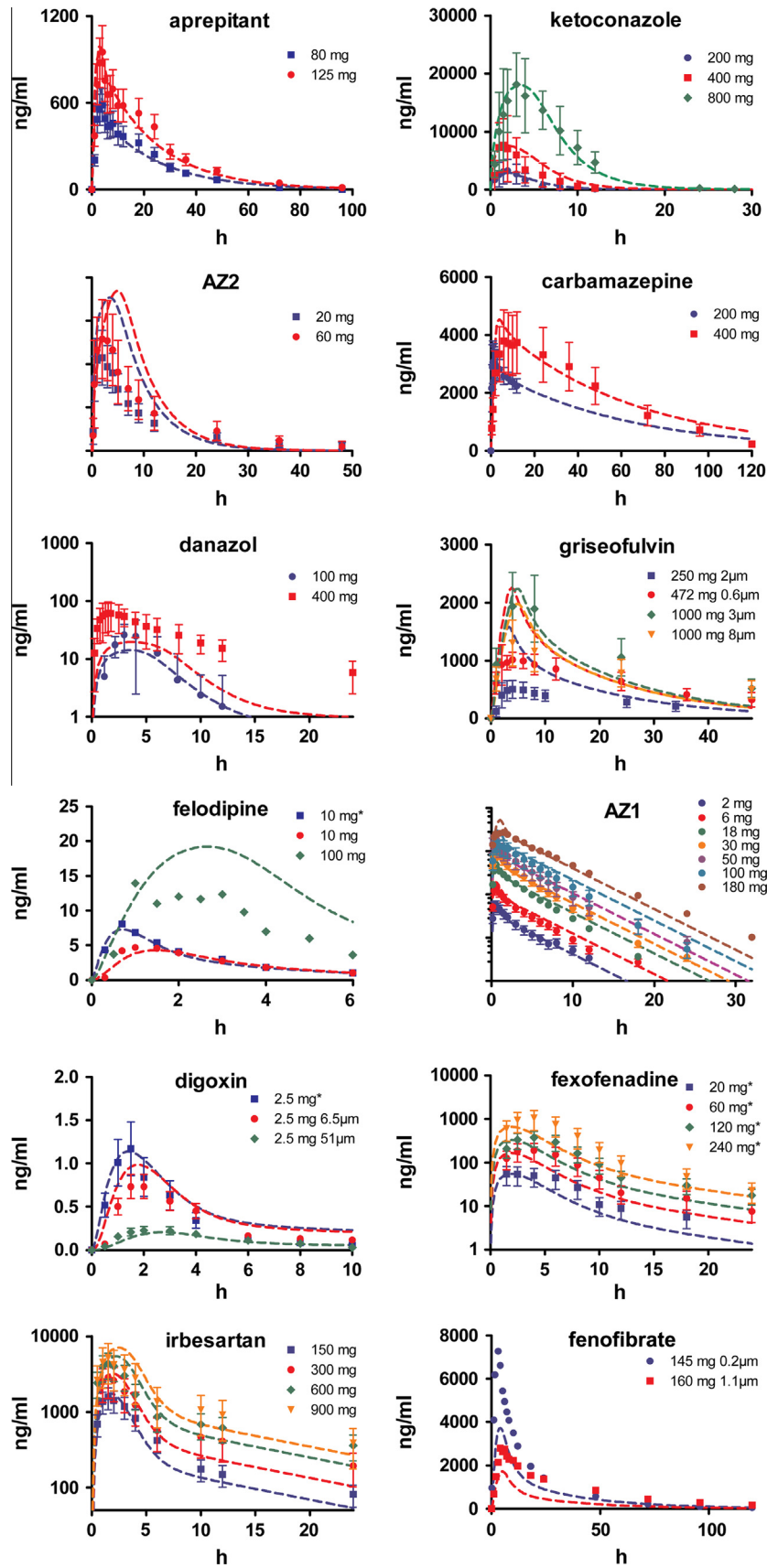


Fig. 5. Plasma concentration profiles. Observed (symbols) and predicted (dotted lines) plasma concentration time profiles of investigated administrations. Plasma concentrations for AZ1 and AZ2 are in arbitrary units due to confidentiality. Administration of solutions are indicated by a star (*). Error in observation is indicated as standard deviation. Linear or log scale of the y-axis was chosen based on best visualization of the plasma profiles. Observed concentration–time data are appended as supplementary data (not for AZ1 and AZ2 due to confidentiality).

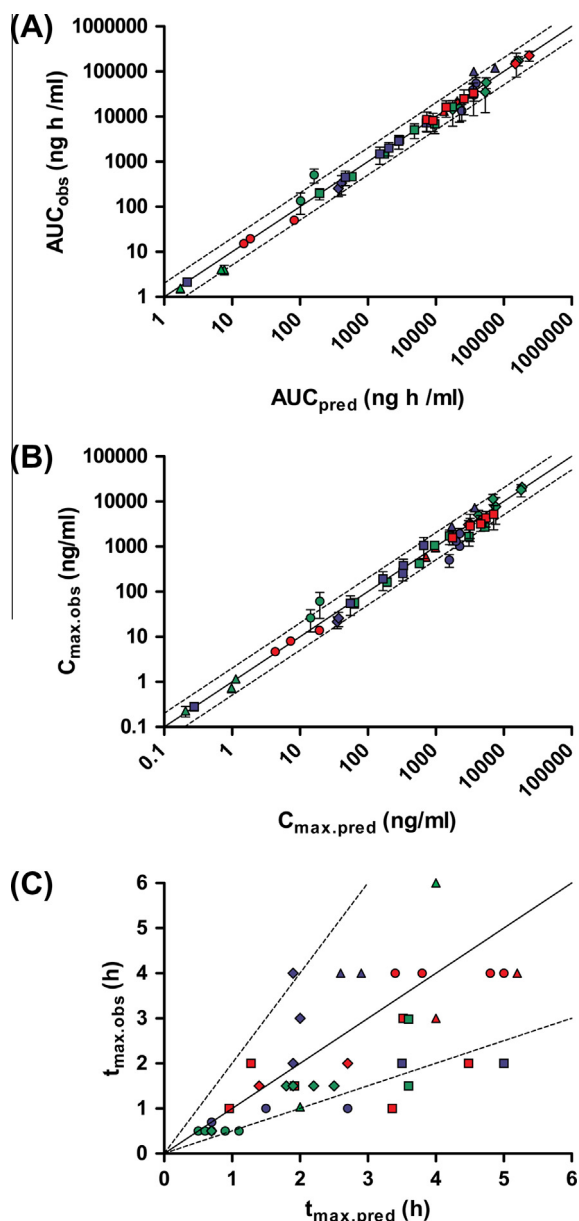


Fig. 6. Overall results. Overview of the overall results from the model API evaluation of GI-Sim. The graphs depict the accuracy in predicted AUC (A), C_{max} (B) and t_{max} (C). Error bars in observed AUC and C_{max} represent standard deviation. Observations in t_{max} are displayed without error due to the discrete character of the parameter. APIs are indicated by color and shape, the solid line and the dotted lines represent the line of unity and a 2-fold difference, respectively.

For instance, the evaluations of the GUT framework, presented by Sugano, and the intestinal supplement to PK-Sim, performed by

Thelen et al., showed 84% ($n = 80$) and 100% ($n = 8$) predictive performance of f_{abs} , respectively (Sugano, 2011; Thelen et al., 2011). Jones et al. applied GASTROPLUS™ in a simulation study and reported the performance level of AUC predictions to be 76% ($n = 21$) whereas the level of accomplishment in the PHRMA initiative for this measurement only was 11% ($n = 18$) (Jones et al., 2011; Poulin et al., 2011). The discrepancy in performance between these studies and models may depend on model differences, e.g., included processes, model structure, system parameters and applied algorithms. However, since the evaluation procedure, e.g., the model APIs included, reference data, what kind of input that is used, as well as the absolute values of the input parameters is different between the studies it is not feasible to make absolute comparisons between the results presented or to compare the predictive performance of the models as such. Also, in some studies parameters, such as gastric pH and regional solubility, was modified making a comparison even more difficult (Parrott et al., 2009; Sugano, 2011). There is currently no report available where a direct head-to-head comparison of the performance of the different absorption simulation software has been made. Such an evaluation would require that simulations are carried out, preferable by the same operator, on the same drugs with identical input for both the drug related biopharmaceutical parameters and the formulation properties.

The use of observed AUC instead of in vivo f_{abs} is associated with potential risks as AUC is affected by additional processes than absorption. Many of the included model APIs are for instance extensively metabolized and substrates for CYP3A4. Hence, there is a risk that the observed AUC also was affected by first-pass gut wall extraction. This potential pre-systemic loss was not accounted for and could lead to an overprediction of AUC, and a misinterpretation of the level of accuracy in predicted f_{abs} . Also, absorption from the colon compartments were excluded in this evaluation since it is known to result in overpredictions of f_{abs} (Kesisoglou and Wu, 2008). Although the extent of colonic absorption in vivo is generally low for APIs with permeability and/or solubility limited absorption (BCS class II, III and IV) due to limited surface area and fluid volume in relation to the small intestine this may in turn result in a bias towards underpredictions (Tannergren et al., 2009). Moreover, transporter-mediated effects may potentially also affect the accuracy in the f_{abs} predictions. Carrier mediated uptake, with significant contribution to f_{abs} , has predominately been shown for molecules with peptide like structures (Brandsch et al., 2008). Whether carrier mediated efflux will effectively reduce f_{abs} , increase the possibility for metabolism or solely reduce the absorption rate and by this delay the absorption process rather than to affect total absorption has been debated (Benet and Cummins, 2001; Pang, 2003). However combined with improved knowledge, the inclusion of intestinal efflux and metabolism functionalities as well as an improved colon model would increase the confidence in the use of GI-Sim as well as potentially increase the accuracy in the predictions of f_{abs} and plasma profiles.

Table 6 Summary of the overall accuracy in the predictions of the pharmacokinetic parameters AUC, C_{max} and t_{max} . The results are shown as percent of the cases in specific accuracy level.

	Level of accuracy(deviation from observation)			
	High (0–25%)	Medium (25–50%)	Low (50%–2-fold)	Inaccurate (>2-fold)
AUC	58	15	22	5
C_{max}	50	23	17	10
t_{max}	28	43	12	17
	High (0–25%)	Medium or higher (0–50%)	Low or higher (0–2-fold)	Inaccurate (>2-fold)
AUC	58	73	95	5
C_{max}	50	73	90	10
t_{max}	28	70	83	17

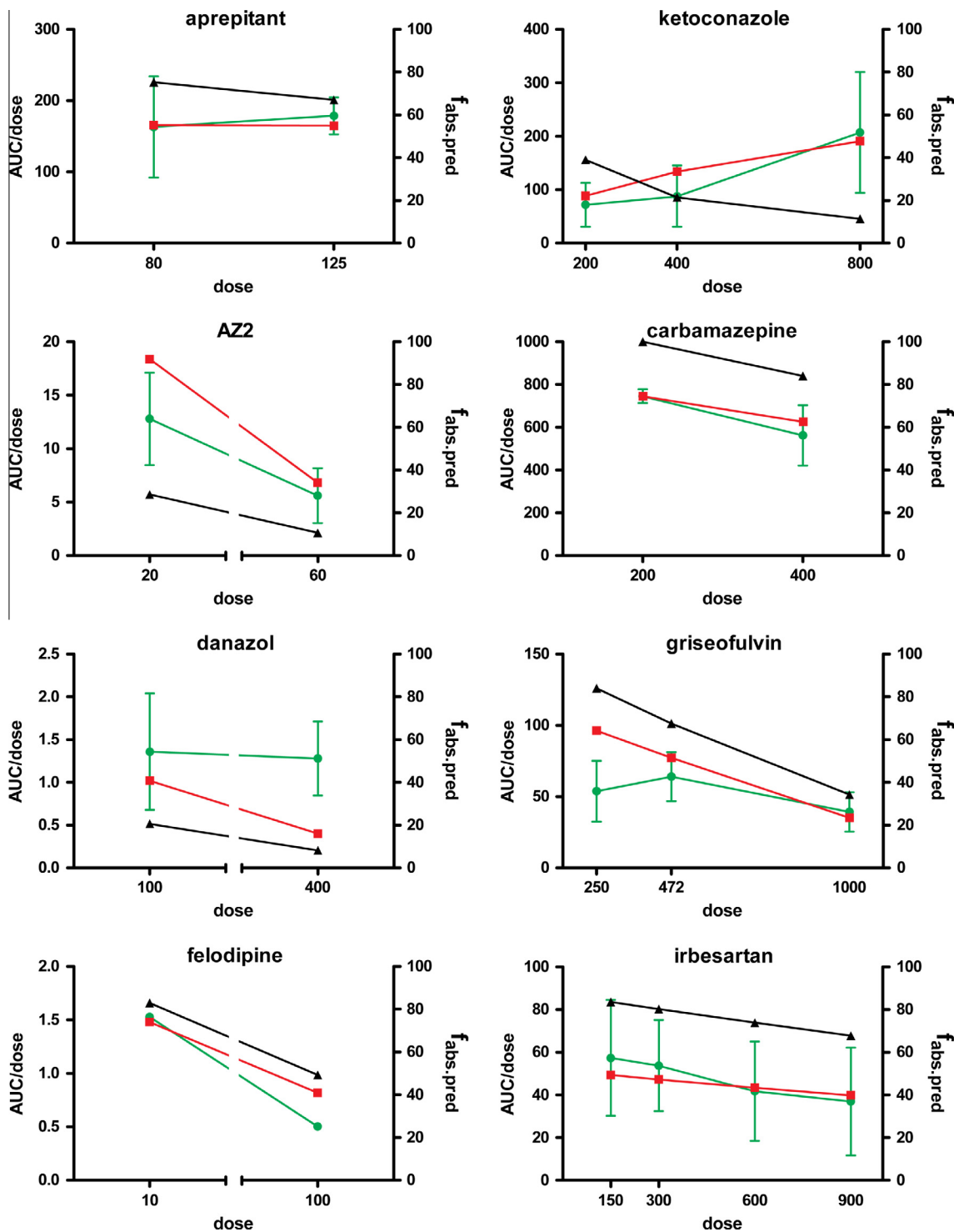


Fig. 7. Dose dependent absorption. Prediction of dose dependent absorption of formulations containing solid material. Observed (green) and predicted (red) AUC (ng h/ml) (arbitrary unit for AZ2 due to confidentiality), normalized to dose (mg), as well as predicted f_{abs} (black) is indicated. Observations are displayed as means with standard deviation. Information of variability was unavailable for felodipine. (For interpretation of the references to color in this figure legend, the reader is referred to the web version of this article.)

5.3.2. Prediction of dose dependent absorption of formulations containing solid material

The observed dose normalized AUC of solid dosage forms of carbamazepine, griseofulvin, danazol, felodipine, irbesartan and AZ2 decreases at higher doses to various degrees as a consequence of a decrease in f_{abs} due to solubility limited absorption. As shown in Fig. 7, the dose dependent absorption of these drugs was well predicted by GI-Sim. In all cases, except danazol, similar trends

in AUC_{pred} as for AUC_{obs} were acquired. No dose dependent absorption has been observed for the low solubility molecule AZ1, and indeed f_{abs} of 100% was predicted by GI-Sim over the studied dose range (Table 5).

GI-Sim was able to properly capture the supra-proportional dose–exposure trend observed for ketoconazole. This was accomplished by a combination of well predicted absorption and the fact that the pharmacokinetic parameters were based upon plasma

concentration–time profiles for solutions at the same doses. Applied CL and distribution volume were hence compensated for bio-availability, i.e., CL/F and V/F . As f_{abs} already were accounted for, the supra-proportional trend was most likely related to dose dependent alteration of gut wall and hepatic first-pass effects, according to $F = f_{abs} \cdot (1 - E_g) \cdot (1 - E_h)$. The clinical data collected for carbamazepine and griseofulvin were related to administration of different doses of formulations with different particle sizes. The result from this study indicates that the absorption of carbamazepine will be sufficiently high provided that the formulation is adequately micronized, which was not the case for the 400 mg dose. The variable prediction success shown for griseofulvin may be a result of incomplete particle size information. The micronization process used for griseofulvin results in a material named microsize or ultramicrosize with a general particle size up to 5 μm (Martin and Tsuk, 1982). This formulation is manufactured by spraydrying API together with polymers, thus making the effective particle size of the API difficult to assess.

The exposure of the nanoparticle formulation of aprepitant was well captured for both doses investigated (80 and 125 mg). It should be noted that aprepitant has been classified as a moderate permeability API in previous studies based on Caco-2 data (Takano et al., 2008; Wu et al., 2004). The same conclusion was made in our lab in the absence of BSA in the basolateral chamber in the Caco-2 permeability assay (data not shown). However, in presence of BSA in the basolateral chamber, the permeability was very high ($P_{app} = 1.7 \times 10^{-4}$ cm/s). This indicates that the moderate permeability measurement is an in vitro artefact likely caused by binding and/or lack of maintained sink condition over the course of the experiment. Error in the permeability input has high impact on the predictive performance and may be one of the reasons for earlier difficulties to attain accurate predictions of in vivo performance of nanoformulations of aprepitant (Kesisoglou and Wu, 2008).

5.3.3. Prediction of particle size dependent absorption

Reference APIs with different particle size for the same solid dose were digoxin, fenofibrate and griseofulvin. Fenofibrate was designated to this investigation as the particle size differences between the available administrations were much larger (0.2–1.9 μm) than the difference in dose (145–160 mg). The observed dose normalized AUC of solid dosage forms of digoxin and fenofibrate decreases when the particle size increases as a consequence of decreased f_{abs} due to dissolution/solubility limited absorption. As shown in Fig. 8, the particle size dependent absorption of digoxin and fenofibrate was well predicted by GI-Sim whereas the effect of particle size was overpredicted for griseofulvin. The latter discrepancy might be due to the formulation process influencing particle size or API form as discussed previously (see Section 5.3.2). The increase in digoxin exposures due to a reduction of particle size were to some extent overpredicted. This can however not be explained by the influence of intestinal P-gp efflux since the exposure of the 51 μm formulation was well predicted. The result for fenofibrate is discussed further below (see Section 5.3.4).

The results presented above (Figs. 5, 7 and 8, Table 5) clearly shows that GI-Sim has the ability to predict dose and particle size dependent absorption in vivo in humans caused by solubility and dissolution limited absorption, respectively. This has practical implications for the clinical formulation development as it may enable early decisions related to the need for micronization or solubility enhanced formulations as well as by reducing cost and development time by avoiding clinical studies, which would fail due to incomplete absorption and too low plasma exposure. The ability of GI-Sim to predict particle size and dose dependency is comparable to previous results reported by Sugano, however it

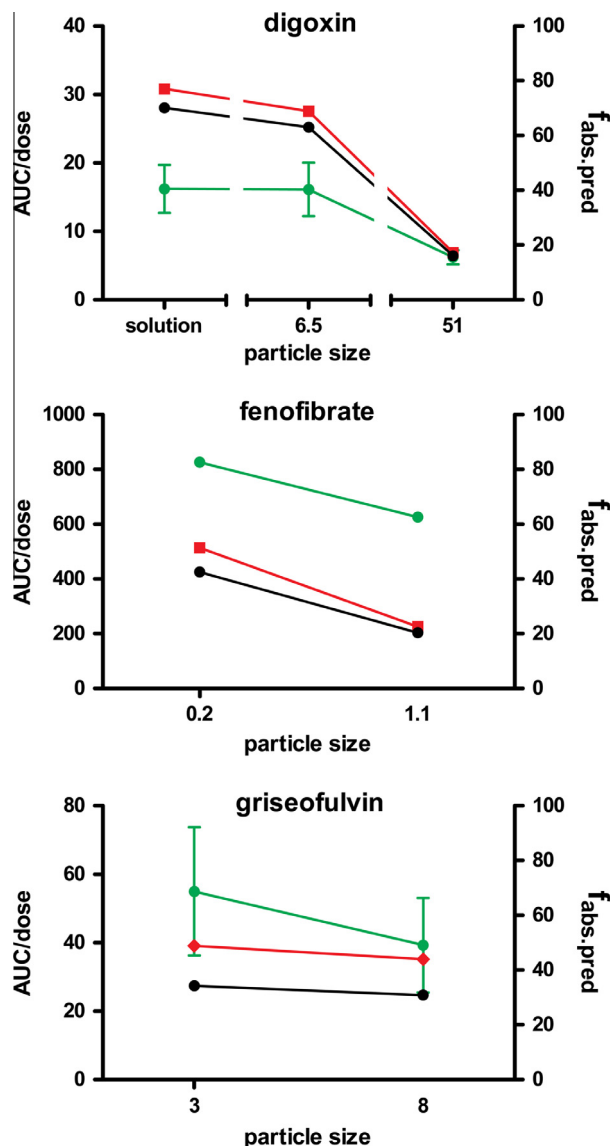


Fig. 8. Particle size dependent absorption. Prediction of particle size dependent absorption. Observed (green) and predicted (red) AUC (ng h/ml), normalized to dose (mg), as well as predicted f_{abs} (black) is indicated. The particle sizes in the plots is the radius given in μm . Observations of are displayed as means with standard deviation. Information of variability was unavailable for fenofibrate. (For interpretation of the references to colour in this figure legend, the reader is referred to the web version of this article.)

should be noted that no parameter optimization was done in this work to achieve the reported results (Sugano, 2011).

5.3.4. Prediction of in vivo performance of nanoformulations

It is well established that nanoformulations can be used to improve the intestinal absorption of low solubility APIs, in particular those classified in BCS Class II. As the development of these formulations are costly and resource demanding, quantitative predictions of f_{abs} and F would be very useful to guide decisions to initiate development of nanoformulation. However, the inability to accurately predict the in vivo performance of nanoformulations has been suggested to be a major limitation for existing absorption models (Kesisoglou and Wu, 2008). Both aprepitant and fenofibrate have been developed as nanoformulations. The predictions of the plasma exposure of aprepitant after administrations of a nanoformulation were excellent (Table 5 and Fig. 5). For fenofibrate, the

relative increase in plasma exposure obtained with a nanoformulation compared to a micronized formulation was well captured by GI-Sim, but the absolute plasma exposure was underpredicted (Table 5 and Fig. 8). The discrepancies in successful outcome may be explained by that high-quality information of particle characteristics and pharmacokinetics was available in the literature for aprepitant but less so for fenofibrate. Previous physiological absorption modeling approaches to simulate the in vivo performance of the nanoformulation of aprepitant in humans have applied regionally adjusted solubility values to enable appropriate simulation of the corresponding plasma profiles of aprepitant (Parrott et al., 2009). In all, GI-Sim has the potential to make accurate predictions of the improvement to the absorption that may be achieved with a nanoformulation.

6. Conclusions

The evaluation of GI-Sim towards clinical reference data for BCS class II, III and IV drugs showed that the predictive performance of oral absorption was high as 95% of the predicted AUC was within a 2-fold deviation to observation. It was also shown that GI-Sim was able to capture the influence of dose and particle size effects, including nanoformulations, on drug absorption. The adequate performance of GI-Sim was also shown in that no influence on the performance was seen between neutral, acid or basic APIs. In all, the outcome is particularly satisfying considering that the selected model APIs are incompletely absorbed. APIs with complete and rapid absorption can generally be readily predicted, with little demands on detailed information and sophisticated algorithms for involved processes.

An essential aspect to the evaluation was that all predictions performed in this study were made with the exact same settings to the software. Adjusting system parameters from case to case is not an option for operational usage and confidence in the result. This modeling approach is also crucial to increase the possibility to re-evaluate previously performed predictions and to analyze large numbers predictions for assessment of general outcome and software performance.

The importance of well determined input parameters like permeability or particle size in the final formulation should also be emphasized. The sensitivity analysis illustrated that the accuracy in predictions for APIs with challenging biopharmaceutical properties is highly dependent on the quality of data. This puts high demand on the methodologies, not only in terms of robustness and sensitivity, but also in the analysis and interpretation of the raw data acquired. The current study illustrated that predictions could be improved by high quality permeability determination. Generation of extended high quality data set in the future is crucial for further validation and improvement of predictive models like GI-Sim. There are also possibilities for further enhanced functionality in the absorption algorithms, for example regarding transformation of solid state forms with different solubility, regional variation of permeability and carrier-mediated transport mechanisms.

In conclusions, the results in the current study are very encouraging showing that useful predictions of intestinal absorption indeed can be obtained, even for challenging APIs, if the adopted model is well characterized and the input data is of high quality. Thus, this could provide useful guidance in the development of oral formulations for challenging molecules leading to increased development efficiency by reducing trial and error approaches.

Financial support

This work was supported by AstraZeneca R&D Mölndal, Mölndal, Sweden.

Appendix A.

The GI-Sim model is here described in a schematic mathematical way. This description is for the case when all particles are considered monodisperse.

The state in compartment i is given by

$X_{sa,i}$ = amount of drug in solid particles given in administration.

$X_{sn,i}$ = amount of drug in solid particles created by nucleation.

$X_{d,i}$ = amount of drug in dissolved form, both in the solution and distributed to micelles.

$N_{sa,i}$ = number of drug solid particles given in administration.

$N_{sn,i}$ = number of drug solid particles created by nucleation.

From the quantities above we can calculate the concentration of dissolved drug in the aqueous phase,

$$C_b = (1 - q) \frac{X_{d,i}}{V_i} \quad (\text{A.1})$$

Here V_i is the volume of compartment i . The average radius of administered and nucleated particles, respectively, is

$$R_{sa,i} = \sqrt[3]{\frac{3X_{sa,i}V_m}{4\pi N_{sa,i}}} \quad (\text{A.2})$$

$$R_{sn,i} = \sqrt[3]{\frac{3X_{sn,i}V_m}{4\pi N_{sn,i}}} \quad (\text{A.3})$$

The pharmacokinetics is described by the amount of drug in central compartment is X_{cc} and in the two peripheral compartments X_2 and X_3 , respectively.

The state in compartment i is changed according to

$$\frac{dX_{sa,i}}{dt} = F_{transit,X_{sa,i}} + F_{growth/dissolution,sa,i} \quad (\text{A.4})$$

$$\frac{dX_{sn,i}}{dt} = F_{transit,X_{sn,i}} + F_{growth/dissolution,sn,i} + F_{nucleation,X_{sn,i}} \quad (\text{A.5})$$

$$\frac{dX_{d,i}}{dt} = F_{transit,X_{d,i}} - F_{growth/dissolution,sa,i} - F_{growth/dissolution,sn,i} - F_{nucleation,X_{sn,i}} - F_{absorption,i} \quad (\text{A.6})$$

$$\frac{dN_{sa,i}}{dt} = F_{transit,N_{sa,i}} \quad (\text{If } X_{sa,i} = 0, \text{ set } N_{sa,i} = 0) \quad (\text{A.7})$$

$$\frac{dN_{sn,i}}{dt} = F_{transit,N_{sn,i}} + F_{nucleation,N_{sn,i}} \quad (\text{If } X_{sn,i} = 0, \text{ set } N_{sn,i} = 0) \quad (\text{A.8})$$

where

$$F_{transit,X_{sa,i}} = \frac{X_{sa,i-1}}{\tau_{i-1}} - \frac{X_{sa,i}}{\tau_i} \quad (\text{A.9})$$

$$F_{transit,X_{sn,i}} = \frac{X_{sn,i-1}}{\tau_{i-1}} - \frac{X_{sn,i}}{\tau_i} \quad (\text{A.10})$$

$$F_{transit,X_{d,i}} = \frac{X_{d,i-1}}{\tau_{i-1}} - \frac{X_{d,i}}{\tau_i} \quad (\text{A.11})$$

$$F_{transit,N_{sa,i}} = \frac{N_{sa,i-1}}{\tau_{i-1}} - \frac{N_{sa,i}}{\tau_i} \quad (\text{A.12})$$

$$F_{transit,N_{sn,i}} = \frac{N_{sn,i-1}}{\tau_{i-1}} - \frac{N_{sn,i}}{\tau_i} \quad (\text{A.13})$$

$$F_{\text{growth/dissolution},sa,i} = 4\pi R_{sa,i} DN_{sa,i} \Psi_{sa,i} (C_{b,i} - S_{b,i}) f_{\text{stirring}}(R_{sa,i}) \quad (\text{A.14})$$

$$F_{\text{growth/dissolution},sn,i} = 4\pi R_{sn,i} DN_{sn,i} \Psi_{sn,i} (C_{b,i} - S_{b,i}) f_{\text{stirring}}(R_{sn,i}) \quad (\text{A.15})$$

$$\Psi = \begin{cases} \frac{R}{R+5 \mu\text{m}} & \text{growth} \\ 1 & \text{dissolution} \end{cases} \quad (\text{A.16})$$

$$F_{\text{absorption},i} = PA_i C_{b,i} \quad (\text{A.17})$$

$$\left. \begin{matrix} F_{\text{nucleation},X_{sn,i}} \\ F_{\text{nucleation},N_{sn,i}} \end{matrix} \right\} \text{Described in Lindfors et al. (2008)} \quad (\text{A.18})$$

Here A_i is the area of compartment i .
Pharmacokinetics is modeled by

$$\frac{dX_{cc}}{dt} = (1 - \text{first pass}) \cdot \sum F_{\text{absorption},i} - \left(k_{12} + k_{13} + \frac{CL}{V_{cc}} \right) X_{cc} + k_{21} X_2 + k_{31} X_3 \quad (\text{A.19})$$

$$\frac{dX_2}{dt} = k_{12} X_{cc} - k_{21} X_2 \quad (\text{A.20})$$

$$\frac{dX_3}{dt} = k_{13} X_{cc} - k_{31} X_3 \quad (\text{A.21})$$

where CL is clearance and V_{cc} is the distribution volume of the central compartment.

Appendix B. Supplementary material

Supplementary data associated with this article can be found, in the online version, at <http://dx.doi.org/10.1016/j.ejps.2013.05.019>.

References

- Aapro, M.S., Walko, C.M., 2010. Aprepitant: drug–drug interactions in perspective. *Ann. Oncol.* 21, 2316–2323.
- Agoram, B., Woltoz, W.S., Bolger, M.B., 2001. Predicting the impact of physiological and biochemical processes on oral drug bioavailability. *Adv. Drug Deliv. Rev.* 50 (Suppl. 1), S41–67.
- Amidon, G.L., Lennernäs, H., Shah, V.P., Crison, J.R., 1995. A theoretical basis for a biopharmaceutical drug classification: the correlation of in vitro drug product dissolution and in vivo bioavailability. *Pharm. Res.* 12, 413–420.
- Avdeef, A., Tam, K.Y., 2010. How well can the Caco-2/Madin-Darby canine kidney models predict effective human jejunal permeability? *J. Med. Chem.* 53, 3566–3584.
- Baarnhielm, C., Backman, A., Hoffmann, K.J., Weidolf, L., 1986. Biotransformation of felodipine in liver microsomes from rat, dog, and man. *Drug Metab. Dispos.* 14, 613–618.
- Badcock, N.R., Bartholomeusz, F.D., Frewin, D.B., Sansom, L.N., Reid, J.G., 1987. The pharmacokinetics of ketoconazole after chronic administration in adults. *Eur. J. Clin. Pharmacol.* 33, 531–534.
- Benet, L., Wu, C., Custodio, J., 2006. Predicting drug absorption and the effects of food on oral bioavailability. *Bull. Techn. Gattefosse*, 9–16.
- Benet, L.Z., Cummins, C.L., 2001. The drug efflux-metabolism alliance: biochemical aspects. *Adv. Drug Deliv. Rev.* 50 (Suppl. 1), S3–11.
- Borgström, L., Nyberg, L., Jonsson, S., Lindberg, C., Paulson, J., 1989. Pharmacokinetic evaluation in man of terbutaline given as separate enantiomers and as the racemate. *Br. J. Clin. Pharmacol.* 27, 49–56.
- Brandsch, M., Knütter, I., Bosse-Doenecke, E., 2008. Pharmaceutical and pharmacological importance of peptide transporters. *J. Pharm. Pharmacol.* 60, 543–585.
- Cagigal, E., Gonzalez, L., Alonso, R.M., Jimenez, R.M., 2001. PK(a) determination of angiotensin II receptor antagonists (ARA II) by spectrofluorimetry. *J. Pharm. Biomed. Anal.* 26, 477–486.
- Carlert, S., Pålsson, A., Hanisch, G., von Corswant, C., Nilsson, C., Lindfors, L., Lennernäs, H., Abrahamsson, B., 2010. Predicting intestinal precipitation – a case example for a basic BCS class II drug. *Pharm. Res.* 27, 2119–2130.
- Chando, T.J., Everett, D.W., Kahle, A.D., Starrett, A.M., Vachharajani, N., Shyu, W.C., Kripalani, K.J., Barbhuiya, R.H., 1998. Biotransformation of irbesartan in man. *Drug Metab. Dispos.* 26, 408–417.
- Charman, W.N., Rogge, M.C., Boddy, A.W., Berger, B.M., 1993. Effect of food and a monoglyceride emulsion formulation on danazol bioavailability. *J. Clin. Pharmacol.* 33, 381–386.

- Chiou, W.L., Chung, S.M., Wu, T.C., Ma, C., 2001. A comprehensive account on the role of efflux transporters in the gastrointestinal absorption of 13 commonly used substrate drugs in humans. *Int. J. Clin. Pharmacol. Ther.* 39, 93–101.
- Chiou, W.L., Riegelman, S., 1971. Absorption characteristics of solid dispersed and micronized griseofulvin in man. *J. Pharm. Sci.* 60, 1376–1380.
- Daneshmend, T.K., Warnock, D.W., Ene, M.D., Johnson, E.M., Potten, M.R., Richardson, M.D., Williamson, P.J., 1984. Influence of food on the pharmacokinetics of ketoconazole. *Antimicrob. Agents Chemother.* 25, 1–3.
- Darwich, A.S., Neuhoff, S., Jamei, M., Rostami-Hodjegan, A., 2010. Interplay of metabolism and transport in determining oral drug absorption and gut wall metabolism: a simulation assessment using the “Advanced Dissolution, Absorption, Metabolism (ADAM)” model. *Curr. Drug Metab.* 11, 716–729.
- Edgar, B., Regårdh, C.G., Johnson, G., Johansson, L., Lundborg, P., Löfberg, I., Rönn, O., 1985. Felodipine kinetics in healthy men. *Clin. Pharmacol. Ther.* 38, 205–211.
- Edwards, F., Tsakmaka, C., Mohr, S., Fielden, P.R., Goddard, N.J., Booth, J., Tam, K.Y., 2013. Using droplet-based microfluidic technology to study the precipitation of a poorly water-soluble weakly basic drug upon a pH-shift. *Analyst* 138, 339–345.
- Fagerholm, U., Lennernäs, H., 1995. Experimental estimation of the effective unstirred water layer thickness in the human jejunum, and its importance in oral-drug absorption. *Eur. J. Pharm. Sci.* 3, 247–253.
- Fenner, K.S., Troutman, M.D., Kempshall, S., Cook, J.A., Ware, J.A., Smith, D.A., Lee, C.A., 2009. Drug–drug interactions mediated through P-glycoprotein: clinical relevance and in vitro-in vivo correlation using digoxin as a probe drug. *Clin. Pharmacol. Ther.* 85, 173–181.
- Greiner, B., Eichelbaum, M., Fritz, P., Kreichgauer, H.P., von Richter, O., Zundler, J., Kroemer, H.K., 1999. The role of intestinal P-glycoprotein in the interaction of digoxin and rifampin. *J. Clin. Invest.* 104, 147–153.
- Hayashi, R., Hilgendorf, C., Artursson, P., Augustijns, P., Brodin, B., Dehertogh, P., Fisher, K., Fossati, L., Hovenkamp, E., Korjamo, T., Masungi, C., Maubon, N., Mols, R., Müllertz, A., Monkkonen, J., O’Driscoll, C., Oppers-Tiemissen, H.M., Ragnarsson, E.G., Rooseboom, M., Ungell, A.L., 2008. Comparison of drug transporter gene expression and functionality in Caco-2 cells from 10 different laboratories. *Eur. J. Pharm. Sci.* 35, 383–396.
- Heikkinen, A.T., Baneyx, G., Caruso, A., Parrott, N., 2012. Application of PBPK modeling to predict human intestinal metabolism of CYP3A substrates – an evaluation and case study using GastroPlus. *Eur. J. Pharm. Sci.* 47, 375–386.
- Hellriegel, E.T., Björnsson, T.D., Hauck, W.W., 1996. Interpatient variability in bioavailability is related to the extent of absorption: implications for bioavailability and bioequivalence studies. *Clin. Pharmacol. Ther.* 60, 601–607.
- Henderson, L.J., 1908. Concerning the relationship between the strength of acids and their capacity to preserve neutrality. *Am. J. Physiol.* 21, 173–179.
- Hogben, C.A., Tocco, D.J., Brodie, B.B., Schanker, L.S., 1959. On the mechanism of intestinal absorption of drugs. *J. Pharmacol. Exp. Ther.* 125, 275–282.
- Hooper, W.D., Eadie, M.J., Dickinson, R.G., 1991. Single oral dose pharmacokinetics and comparative bioavailability of danazol in humans. *Biopharm. Drug Dispos.* 12, 577–582.
- Huang, Y.C., Colaizzi, J.L., Bierman, R.H., Woestenborghs, R., Heykants, J., 1986. Pharmacokinetics and dose proportionality of ketoconazole in normal volunteers. *Antimicrob. Agents Chemother.* 30, 206–210.
- Igel, S., Drescher, S., Murdter, T., Hofmann, U., Heinkele, G., Tegude, H., Glaeser, H., Brenner, S.S., Somogyi, A.A., Omari, T., Schäfer, C., Eichelbaum, M., Fromm, M.F., 2007. Increased absorption of digoxin from the human jejunum due to inhibition of intestinal transporter-mediated efflux. *Clin. Pharmacokinet.* 46, 777–785.
- Jalava, K.M., Olkkola, K.T., Neuvonen, P.J., 1997. Itraconazole greatly increases plasma concentrations and effects of felodipine. *Clin. Pharmacol. Ther.* 61, 410–415.
- Jiang, W., Kim, S., Zhang, X., Lionberger, R.A., Davit, B.M., Conner, D.P., Yu, L.X., 2011. The role of predictive biopharmaceutical modeling and simulation in drug development and regulatory evaluation. *Int. J. Pharm.* 418, 151–160.
- Jones, H.M., Gardner, I.B., Collard, W.T., Stanley, P.J., Oxley, P., Hosea, N.A., Plowchalk, D., Gernhardt, S., Lin, J., Dickens, M., Rahavendran, S.R., Jones, B.C., Watson, K.J., Pertinez, H., Kumar, V., Cole, S., 2011. Simulation of human intravenous and oral pharmacokinetics of 21 diverse compounds using physiologically based pharmacokinetic modelling. *Clin. Pharmacokinet.* 50, 331–347.
- Jounela, A.J., Pentikainen, P.J., Sothmann, A., 1975. Effect of particle size on the bioavailability of digoxin. *Eur. J. Clin. Pharmacol.* 8, 365–370.
- Jönsson, S., Henningson, A., Edholm, M., Salmonson, T., 2012. Role of modelling and simulation: a European regulatory perspective. *Clin. Pharmacokinet.* 51, 69–76.
- Kansy, M., Senner, F., Gubernator, K., 1998. Physicochemical high throughput screening: parallel artificial membrane permeation assay in the description of passive absorption processes. *J. Med. Chem.* 41, 1007–1010.
- Karlsson, J., Artursson, P., 1991. A method for the determination of cellular permeability coefficients and aqueous boundary-layer thickness in monolayers of intestinal epithelial (Caco-2) cells grown in permeable filter chambers. *Int. J. Pharm.* 71, 55–64.
- Kerr, B.M., Thummel, K.E., Wurden, C.J., Klein, S.M., Kroetz, D.L., Gonzalez, F.J., Levy, R.H., 1994. Human liver carbamazepine metabolism. Role of CYP3A4 and CYP2C8 in 10,11-epoxide formation. *Biochem. Pharmacol.* 47, 1969–1979.
- Kesisoglou, F., Wu, Y., 2008. Understanding the effect of API properties on bioavailability through absorption modeling. *AAPS J.* 10, 516–525.
- Konishi, H., Takenaka, A., Minouchi, T., Yamaji, A., 2001. Impairment of CYP3A4 capacity in patients receiving danazol therapy: examination on oxidative cortisol metabolism. *Horm. Metab. Res.* 33, 628–630.

- Kotlarchyk, M., Stephens, R.B., Huang, J.S., 1988. Study of Schultz distribution to model polydispersity of microemulsion droplets. *J. Phys. Chem. – US* 92, 1533–1538.
- Kovacevic, I., Parojcic, J., Homsek, I., Tubic-Grozdanis, M., Langguth, P., 2009. Justification of biowaiver for carbamazepine, a low soluble high permeable compound, in solid dosage forms based on IVVC and gastrointestinal simulation. *Mol. Pharm.* 6, 40–47.
- Lancaster, S.G., Todd, P.A., 1988. Lisinopril. A preliminary review of its pharmacodynamic and pharmacokinetic properties, and therapeutic use in hypertension and congestive heart failure. *Drugs* 35, 646–669.
- Lappin, G., Shishikura, Y., Jochemsen, R., Weaver, R.J., Gesson, C., Houston, B., Oosterhuis, B., Bjerrum, O.J., Rowland, M., Garner, C., 2010. Pharmacokinetics of fexofenadine: evaluation of a microdose and assessment of absolute oral bioavailability. *Eur. J. Pharm. Sci.* 40, 125–131.
- Lennernas, H., 2007. Intestinal permeability and its relevance for absorption and elimination. *Xenobiotica* 37, 1015–1051.
- Lin, C., Symchowicz, S., 1975. Absorption, distribution, metabolism, and excretion of griseofulvin in man and animals. *Drug Metab. Rev.* 4, 75–95.
- Lin, C.C., Magat, J., Chang, R., McGlotten, J., Symchowicz, S., 1973. Absorption, metabolism and excretion of 14C-griseofulvin in man. *J. Pharmacol. Exp. Ther.* 187, 415–422.
- Lindfors, L., Forssen, S., Westergren, J., Olsson, U., 2008. Nucleation and crystal growth in supersaturated solutions of a model drug. *J. Colloid Interface Sci.* 325, 404–413.
- Löbenberg, R., Amidon, G.L., 2000. Modern bioavailability, bioequivalence and biopharmaceutics classification system. New scientific approaches to international regulatory standards. *Eur. J. Pharm. Biopharm.* 50, 3–12.
- Majumdar, A.K., Howard, L., Goldberg, M.R., Hickey, L., Constanzer, M., Rothenberg, P.L., Crumley, T.M., Panebianco, D., Bradstreet, T.E., Bergman, A.J., Waldman, S.A., Greenberg, H.E., Butler, K., Knops, A., De Lepeleire, I., Michiels, N., Petty, K.J., 2006. Pharmacokinetics of aprepitant after single and multiple oral doses in healthy volunteers. *J. Clin. Pharmacol.* 46, 291–300.
- Marino, M.R., Langenbacher, K., Ford, N.F., Uderman, H.D., 1998. Pharmacokinetics and pharmacodynamics of irbesartan in healthy subjects. *J. Clin. Pharmacol.* 38, 246–255.
- Martin, F.H., Tsuk, A.G., 1982. Therapeutic Compositions with Enhanced Bioavailability. American Home Products Corporation, US, New York.
- Marvel, J.R., Schlichting, D.A., Denton, C., Levy, E.J., Cahn, M.M., 1964. The effect of a surfactant and of particle size on griseofulvin plasma levels. *J. Invest. Dermatol.* 42, 197–203.
- Mazer, N.A., Benedek, G.B., Carey, M.C., 1980. Quasielastic light-scattering studies of aqueous biliary lipid systems. Mixed micelle formation in bile salt–lecithin solutions. *Biochemistry* 19, 601–615.
- Ming, X., Knight, B.M., Thakker, D.R., 2011. Vectorial transport of fexofenadine across Caco-2 cells: involvement of apical uptake and basolateral efflux transporters. *Mol. Pharm.* 8, 1677–1686.
- Mudie, D.M., Amidon, G.L., Amidon, G.E., 2010. Physiological parameters for oral delivery and in vitro testing. *Mol. Pharm.*
- Müllertz, A., Fatouros, D.G., Smith, J.R., Vertzoni, M., Reppas, C., 2012. Insights into intermediate phases of human intestinal fluids visualized by atomic force microscopy and cryo-transmission electron microscopy ex vivo. *Mol. Pharmaceut.* 9, 237–247.
- Nawroth, T., Buch, P., Buch, K., Langguth, P., Schweins, R., 2011. Liposome formation from bile salt–lipid micelles in the digestion and drug delivery model FASSI(mod) estimated by combined time-resolved neutron and dynamic light scattering. *Mol. Pharm.* 8, 2162–2172.
- Nielsen, A.E., 1961. Diffusion controlled growth of a moving sphere. The kinetics of crystal growth in potassium perchlorate precipitation. *J. Phys. Chem.* 65, 46–49.
- Ochs, H.R., Bodem, G., Greenblatt, D.J., 1981. Effect of dose on bioavailability of oral digoxin. *Eur. J. Clin. Pharmacol.* 19, 53–55.
- Ochs, H.R., Greenblatt, D.J., Bodem, G., Harmatz, J.S., 1978. Dose-independent pharmacokinetics of digoxin in humans. *Am. Heart J.* 96, 507–511.
- Otte, A., Carvajal, M.T., 2011. Assessment of milling-induced disorder of two pharmaceutical compounds. *J. Pharm. Sci.* 100, 1793–1804.
- Pang, K.S., 2003. Modeling of intestinal drug absorption: roles of transporters and metabolic enzymes (for the Gillette Review Series). *Drug Metab. Dispos.* 31, 1507–1519.
- Parrott, N., Lave, T., 2008. Applications of physiologically based absorption models in drug discovery and development. *Mol. Pharm.* 5, 760–775.
- Parrott, N., Lukacova, V., Fraczkiewicz, G., Bolger, M.B., 2009. Predicting pharmacokinetics of drugs using physiologically based modeling – application to food effects. *AAPS J.* 11, 45–53.
- Pelkonen, O., Turpeinen, M., Hakkola, J., Honkakoski, P., Hukkanen, J., Raunio, H., 2008. Inhibition and induction of human cytochrome P450 enzymes: current status. *Arch. Toxicol.* 82, 667–715.
- Persson, E.M., Gustafsson, A.S., Carlsson, A.S., Nilsson, R.G., Knutson, L., Forsell, P., Hanisch, G., Lennernas, H., Abrahamsson, B., 2005. The effects of food on the dissolution of poorly soluble drugs in human and in model small intestinal fluids. *Pharm. Res.* 22, 2141–2151.
- Petri, N., Borgia, O., Nyberg, L., Hedeland, M., Bondesson, U., Lennernas, H., 2006. Effect of erythromycin on the absorption of fexofenadine in the jejunum, ileum and colon determined using local intubation in healthy volunteers. *Int. J. Clin. Pharmacol. Ther.* 44, 71–79.
- Petri, N., Tannergren, C., Rungstad, D., Lennernas, H., 2004. Transport characteristics of fexofenadine in the Caco-2 cell model. *Pharm. Res.* 21, 1398–1404.
- Poulin, P., Jones, R.D., Jones, H.M., Gibson, C.R., Rowland, M., Chien, J.Y., Ring, B.J., Adkison, K.K., Ku, M.S., He, H., Vuppugalla, R., Marathe, P., Fischer, V., Dutta, S., Sinha, V.K., Bjornsson, T., Lave, T., Yates, J.W., 2011. PHRMA CPDCC initiative on predictive models of human pharmacokinetics, part 5: prediction of plasma concentration–time profiles in human by using the physiologically-based pharmacokinetic modeling approach. *J. Pharm. Sci.*
- Psachoulas, D., Vertzoni, M., Goumas, K., Kalioras, V., Beato, S., Butler, J., Reppas, C., 2011. Precipitation in and supersaturation of contents of the upper small intestine after administration of two weak bases to fasted adults. *Pharm. Res.* 28, 3145–3158.
- Robbins, D.K., Castles, M.A., Pack, D.J., Bhargava, V.O., Weir, S.J., 1998. Dose proportionality and comparison of single and multiple dose pharmacokinetics of fexofenadine (MDL 16455) and its enantiomers in healthy male volunteers. *Biopharm. Drug Dispos.* 19, 455–463.
- Sanchez, R.L., Wang, R.W., Newton, D.J., Bakhtiar, R., Lu, P., Chiu, S.H., Evans, D.C., Huskey, S.E., 2004. Cytochrome P450 3A4 is the major enzyme involved in the metabolism of the substance P receptor antagonist aprepitant. *Drug Metab. Dispos.* 32, 1287–1292.
- Sauron, R., Wilkins, M., Jessent, V., Dubois, A., Maillot, C., Weil, A., 2006. Absence of a food effect with a 145 mg nanoparticle fenofibrate tablet formulation. *Int. J. Clin. Pharmacol. Ther.* 44, 64–70.
- Schiller, C., Frohlich, C.P., Giessmann, T., Siegmund, W., Monnikes, H., Hosten, N., Weitschies, W., 2005. Intestinal fluid volumes and transit of dosage forms as assessed by magnetic resonance imaging. *Aliment. Pharm. Therap.* 22, 971–979.
- Shimizu, M., Fuse, K., Okudaira, K., Nishigaki, R., Maeda, K., Kusuhara, H., Sugiyama, Y., 2005. Contribution of OATP (organic anion-transporting polypeptide) family transporters to the hepatic uptake of fexofenadine in humans. *Drug Metab. Dispos.* 33, 1477–1481.
- Skiba, M., Skiba-Lahiani, M., Marchais, H., Duclos, R., Arnaud, P., 2000. Stability assessment of ketoconazole in aqueous formulations. *Int. J. Pharm.* 198, 1–6.
- Straughn, A.B., Meyer, M.C., Raghov, G., Rotenberg, K., 1980. Bioavailability of microsize and ultramicrosize griseofulvin products in man. *J. Pharmacokin. Biopharm.* 8, 347–362.
- Sugano, K., 2009. Introduction to computational oral absorption simulation. *Expert Opin. Drug Metab. Toxicol.* 5, 259–293.
- Sugano, K., 2011. Fraction of a dose absorbed estimation for structurally diverse low solubility compounds. *Int. J. Pharm.* 405, 79–89.
- Sunesen, V.H., Vedelsdal, R., Kristensen, H.G., Christrup, L., Müllertz, A., 2005. Effect of liquid volume and food intake on the absolute bioavailability of danazol, a poorly soluble drug. *Eur. J. Pharm. Sci.* 24, 297–303.
- Söderlind, E., Karlsson, E., Carlsson, A., Kong, R., Lenz, A., Lindborg, S., Sheng, J.J., 2010. Simulating fasted human intestinal fluids: understanding the roles of lecithin and bile acids. *Mol. Pharm.*
- Takano, R., Furumoto, K., Shiraki, K., Takata, N., Hayashi, Y., Aso, Y., Yamashita, S., 2008. Rate-limiting steps of oral absorption for poorly water-soluble drugs in dogs; prediction from a miniscale dissolution test and a physiologically-based computer simulation. *Pharm. Res.* 25, 2334–2344.
- Tannergren, C., Bergendal, A., Lennernas, H., Abrahamsson, B., 2009. Toward an increased understanding of the barriers to colonic drug absorption in humans: implications for early controlled release candidate assessment. *Mol. Pharm.* 6, 60–73.
- Tannergren, C., Knutson, T., Knutson, L., Lennernas, H., 2003. The effect of ketoconazole on the in vivo intestinal permeability of fexofenadine using a regional perfusion technique. *Br. J. Clin. Pharmacol.* 55, 182–190.
- Thelen, K., Coboeken, K., Willmann, S., Burghaus, R., Dressman, J.B., Lippert, J., 2011. Evolution of a detailed physiological model to simulate the gastrointestinal transit and absorption process in humans, part 1: oral solutions. *J. Pharm. Sci. – US* 100, 5324–5345.
- Uno, T., Shimizu, M., Sugawara, K., Tateishi, T., 2006. Lack of dose-dependent effects of itraconazole on the pharmacokinetic interaction with fexofenadine. *Drug Metab. Dispos.* 34, 1875–1879.
- Vachharajani, N.N., Shyu, W.C., Chando, T.J., Everett, D.W., Greene, D.S., Barbhuiya, R.H., 1998. Oral bioavailability and disposition characteristics of irbesartan, an angiotensin antagonist, in healthy volunteers. *J. Clin. Pharmacol.* 38, 702–707.
- Weil, A., Caldwell, J., Strolin-Benedetti, M., 1990. The metabolism and disposition of 14C-fenofibrate in human volunteers. *Drug Metab. Dispos.* 18, 115–120.
- Willmann, S., Schmitt, W., Keldenich, J., Lippert, J., Dressman, J.B., 2004. A physiological model for the estimation of the fraction dose absorbed in humans. *J. Med. Chem.* 47, 4022–4031.
- Vogt, M., Kunath, K., Dressman, J.B., 2008. Dissolution enhancement of fenofibrate by micronization, cogrinding and spray-drying: comparison with commercial preparations. *Eur. J. Pharm. Biopharm.* 68, 283–288.
- Wu, Y., Loper, A., Landis, E., Hettrick, L., Novak, L., Lynn, K., Chen, C., Thompson, K., Higgins, R., Batra, U., Shelukar, S., Kwei, G., Storey, D., 2004. The role of biopharmaceutics in the development of a clinical nanoparticle formulation of MK-0869: a Beagle dog model predicts improved bioavailability and diminished food effect on absorption in human. *Int. J. Pharm.* 285, 135–146.
- Yasui-Furukori, N., Uno, T., Sugawara, K., Tateishi, T., 2005. Different effects of three transporting inhibitors, verapamil, cimetidine, and probenecid, on fexofenadine pharmacokinetics. *Clin. Pharmacol. Ther.* 77, 17–23.
- Yu, L.X., Amidon, G.L., 1998. Saturable small intestinal drug absorption in humans: modeling and interpretation of cefatrizine data. *Eur. J. Pharm. Biopharm.* 45, 199–203.
- Yu, L.X., Amidon, G.L., 1999. A compartmental absorption and transit model for estimating oral drug absorption. *Int. J. Pharm.* 186, 119–125.

- Yu, L.X., Crison, J.R., Amidon, G.L., 1996. Compartmental transit and dispersion model analysis of small intestinal transit flow in humans. *Int. J. Pharm.* 140, 111–118.
- Zhang, X., Lionberger, R.A., Davit, B.M., Yu, L.X., 2011. Utility of physiologically based absorption modeling in implementing quality by design in drug development. *AAPS J.* 13, 59–71.
- Zhao, P., Rowland, M., Huang, S.M., 2012. Best practice in the use of physiologically based pharmacokinetic modeling and simulation to address clinical pharmacology regulatory questions. *Clin. Pharmacol. Ther.* 92, 17–20.
- Zhu, T., Ansquer, J.C., Kelly, M.T., Sleep, D.J., Pradhan, R.S., 2010. Comparison of the gastrointestinal absorption and bioavailability of fenofibrate and fenofibric acid in humans. *J. Clin. Pharmacol.* 50, 914–921.
- Zimm, B.H., 1948. Apparatus and methods for measurement and interpretation of the angular variation of light scattering – preliminary results on polystyrene solutions. *J. Chem. Phys.* 16, 1099–1116.